A M U L T I - L E V E L M O D E L

OF THE PLANETARY BOUNDARY LAYER SUITABLE FOR USE WITH MESOSCALE DYNAMIC MODELS

B Y

N I E L S E. B U S C H
RESEARCH ESTABLISHMENT RISØ
ROSKILDE, DENMARK

SIMON W. CHANG
RICHARD A. ANTHES
THE PENNSYLVANIA STATE UNIVERSITY

1. Introduction

The major sink of momentum and sources of heat and moisture are at the earth-atmosphere's interface. The vertical fluxes of momentum, heat and moisture are, therefore, usually largest in the planetary boundary layer (PBL), and considerable effort has been directed toward the understanding of this relatively thin layer next to the earth's surface. Many PBL-models of varying complexity have been developed with the purpose of studying the details of the physical processes in this layer alone. However, the treatment of the PBL is also an important part of numerical models of mesoscale or large-scale atmospheric phenomena. In such models, the behavior of the PBL itself is often of secondary interest; what is required is an adequate representation of the coupling between the PBL and the atmospheric flow in the rest of the model.

The degree of accuracy and the detail of the PBL to be resolved in a dynamic model depend mainly on the characteristics of the phenomenon to be modeled. For example, the short-range behavior of the quasi-geostrophic waves in the westerlies may be modeled without any representation of the PBL at all. In long-term integrations of the general circulation, or if the behavior of individual cyclones and smaller scale phenomena is being investigated, the PBL becomes more important. In some of these latter models, the detailed structure of the PBL is unimportant and only its gross effect needs to be considered. In others, a more detailed representation of the PBL is necessary.

2. Approaches to the Boundary Layer Modeling Problem

In most models, the atmospheric boundary layer is divided into a surface boundary-layer next to the ground or sea surface, in which the fluxes of heat, momentum, and water vapor are considered approximately constant with height, and a deeper layer in which these fluxes decrease with height. In general, two approaches are possible toward the incorporation of the effects of the boundary layer into a large-scale model, as discussed by Clarke (1970) and Deardorff (1972b). One is to resolve the structure of the boundary layer explicitly by including several computational levels within the boundary layer. The second method is to relate the gross effects of the PBL to a number of parameters derived from the dynamic large-scale model. As an example of the second approach, Deardorff (1972b) proposes a relatively sophisticated bulk parameterization of the PBL in which the surface stress and the surface fluxes of heat and moisture vary as functions of a bulk Richardson number which is determined from the large-scale model. In this scheme, an important quantity is a time-dependent height, h, of the PBL, which is predicted explicitly.

If the detailed structure of the PBL is important in the dynamical model, the turbulent fluxes of momentum, heat and moisture must be resolved at several levels within the PBL. The difficulty lies in relating these fluxes to the large-scale mean variables that are predicted by the model. Two types of closure

have been attempted. Most investigators have utilized first-order closure schemes, which relate the turbulent fluxes to gradients of the mean quantities through eddy coefficients (e.g., Estoque, 1973). These schemes are economical but suffer from the absence of an accepted formulation of the diffusivities that applies under general conditions.

Recently attempts have been made at the development of higher-order closure schemes (Donaldson, 1973; Lumley and Khajeh-Nouri, 1974; Wyngaard et al., 1974). The closure problem in these schemes is the modeling of the third order moments. Although the second-order closure schemes are intellectually appealing, they do not yet appear to be ready for use in large-scale dynamical models. At present, the second-order closure schemes are controversial, and a large number of constants remain to be determined. A practical limitation at the present is the amount of computer time and storage necessary for these schemes. For example, the boundary layer model of Wyngaard et al. consists of 14 equations, twice as many as normally required in a dynamical model. Thus, in spite of the long-range benefits which may be derived from higher-order schemes, there remains a need in numerical models for simple schemes that produce results consistent with the known behavior of the PBL.

After establishing a need for relatively detailed representation of the boundary layers in hurricane models, we present a simple, time-dependent model of the PBL suitable for use in dynamical models. Preliminary results from this model are encouraging, and suggest that it be tested against real data and higher-order closure schemes as they become available.

3. The Need for Simple, High Resolution PBL Models for Hurricane Studies

One phenomenon which is strongly dependent not only on the gross effects of the PBL, but probably also on the details of the boundary layer structure is the hurricane. It is in the hurricane boundary layer that friction destroys the gradient wind balance and produces the inflow branch of the circulation. This inflow produces the tangential circulation through conservation of the angular momentum, and provides the convergence of water vapor that supports the cumulus convection. Thus, in contrast to many other atmospheric phenomena in which the boundary layer effects are secondary in importance, the boundary layer is critical to the development and maintenance of the hurricane.

Tropical cyclones have been realistically simulated by numerical models (e.g., Ooyama, 1969; Rosenthal, 1970, Anthes, 1972). The structure of these model storms agree remarkably well with the structure of typical hurricanes, in spite of the crude parameterizations of the PBL, including the vital sea-air interactions. However, the intensities of these model hurricanes show an unrealistically strong dependence upon the temperature of the underlying ocean, which supplies crucial heat and water vapor to the storm. This may be due to the greatly simplified treatment of the PBL employed in the models. Both the surface and the

boundary layers are contained in a single, approximately 1-km thick layer. The surface stresses are computed from the quadratic stress law, and the surface fluxes of heat and moisture are calculated from bulk aerodynamic formulas. Under the assumptions that the fluxes of momentum, heat and moisture vanish at the top of the layer, the frictional force and the rate of addition of heat and moisture to the model's lowest layer are obtained.

Although this simple approach apparently accounts for the effects of the PBL to a sufficient degree to obtain fairly realistic model hurricanes, a number of defects in the scheme makes improved treatment of the PBL desirable in order to more realistically model the interactions between the hurricane and the ocean. One difficulty is the assumption of a boundary layer of constant height, which is determined by the choice of the lowest computational level in the model.

In reality, the depth of the boundary layer varies both in time and space during the lifetime of the hurricane, although the degree of variability is not well known. A second important defect in the one-layer parameterization scheme is the crude dependence of the turbulent surface-fluxes of heat, moisture and momentum on static stability, wind shear, and state of the sea surface. In reality,these fluxes will be significantly dependent on the details of the PBL such as the stability of the surface boundary layer (Deardorff, 1972b). This dependence may be very significant for the modification of hurricanes which move over water of varying temperature, or as the ocean temperatures change in response to the hurricane.

Finally, even if the above formulation correctly predicts the vertically averaged properties of the hurricane boundary layer, the details of the structure are missing entirely. A better resolution of the strong vertical gradients of temperature, moisture and wind is becoming more important as cumulus parameterization schemes are improved.

The importance of vertical resolution may be illustrated by the variation of mixing ratio, r, with height. In the mature hurricane, r varies from about 18.7 gm kg^{-1} at 1000 mb to 14.0 gm kg^{-1} at 850 mb (Sheets, 1969). In addition, the vertical shear of the radial (inflow) component of the wind is a maximum in the PBL. Thus an accurate representation of the horizontal water vapor convergence, which is vital to the cumulus convection, requires improvement in the vertical resolution.

In the next section, a simple model of the PBL is proposed which appears suitable for a more realistic simulation of the detailed structure of the hurricane boundary layer. Although designed with some of the hurricane problems in mind, the scheme is general and should be suitable for use in a wide variety of atmospheric models.

4. A Time-Dependent Model of the Planetary Boundary Layer

For simplicity, only one dimension is considered in this

model; the extension to two or three dimensions is straightforward by the inclusion of horizontal advective effects, as long as the small-scale, turbulent structure of the PBL can be considered horizontally quasi-homogenous at each grid-point. The equations of motion and the thermodynamic equation then are

$$\frac{\partial u}{\partial t} = f(v - v_g) - \frac{1}{\rho}\frac{\partial}{\partial z}\overline{\rho u' w'} \tag{1}$$

$$\frac{\partial v}{\partial t} = f(u_g - u) - \frac{1}{\rho}\frac{\partial}{\partial z}\overline{\rho v' w'} \tag{2}$$

$$\frac{\partial T}{\partial t} = -\frac{1}{\rho}\frac{\partial \overline{\rho w' T'}}{\partial z}\ , \tag{3}$$

where the symbols have their usual meteorological meaning and fluctuations in density have been neglected. We now consider the eddy flux terms in the surface layer and in the PBL between the top of the surface layer and the base of a capping inversion.

a. The Surface Layer

The structure of the surface layer is relatively well-known. Here, the lowest 10 m of the PBL are assumed to be within the surface layer, and the nondimensional gradients of wind and potential temperature are solved from similarity theory:

$$\frac{u}{u_{*_o}} = \frac{1}{k}\left[\ln (z/z_o) - \psi_m (z/L)\right] \tag{4}$$

$$\frac{\theta - \theta_o}{\theta_{*_o}} = \left[\ln z/z_o - \psi_h (z/L)\right]\ , \tag{5}$$

where L is the Monin-Obukhov length, defined by

$$L = -\frac{c_p \rho T_o u_{*_o}^3}{kg\ H_o} \qquad H_o = -\rho c_p u_* \theta_*$$

with H_o and $\rho u_{*_o}^2$ being the surface fluxes of heat and momentum, respectively. The functions ψ_m and ψ_h are integrals of universal functions Φ_m and Φ_h as given by Businger (1973). Then the fluxes of momentum and heat in the surface layer can be derived from

$$- \overline{u'w'} = u_{*_o}^2 \left|\frac{\partial u}{\partial z}\right| \Big/ \left|\frac{\partial \vec{v}}{\partial z}\right| \qquad (7)$$

$$- \overline{v'w'} = u_{*_o}^2 \left|\frac{\partial v}{\partial z}\right| \Big/ \left|\frac{\partial \vec{v}}{\partial z}\right| \qquad (8)$$

$$\overline{w'T'} = - u_* \theta_{*_o} = H_o/(c_p \rho) \ . \qquad (9)$$

The calculation marches forward in the following way. First, an initial guess of L is estimated from the values of u_{*_o} and θ_{*_o} at time $t_o - \Delta t$. This value of L is used in (4) and (5) to estimate u_{*_o} and θ_{*_o} at time t_o, which are then used to calculate an updated value of L. This iterative procedure continues until the solution converges.

b. The PBL Above the Surface Layer

Some preliminary efforts were directed toward quasi-stationary modeling of the PBL above the surface layer by use of mixing lengths which approach constant values with increasing heights above the surface (e.g., Panofsky, 1973; p. 153). The efforts included attempts at modification of the mixing lengths for adiabatic cases, so that in the surface boundary layer, the behavior of the wind and temperature profiles would be in accordance with Businger et al. (1971).

A conceptual difficulty in this approach is that the turbulent fluxes at great heights above the surface layer depend directly and instantaneously on the surface layer characteristics, mainly the surface heat flux. The approach failed to treat realistically the effect of a capping inversion, and the behavior of the atmosphere across and above such an inversion. Furthermore, the model predicted unlimited growth of the PBL. These results suggest that the mixing length above the surface layer should explicitly depend on the local conditions and on the height of the capping inversion.

We first define a mixing length, λ, which is the scale of the energy-containing eddies, by

$$u_*^2 \equiv \lambda^2 \left|\frac{\partial \vec{v}}{\partial z}\right|^2 \equiv K_m \left|\frac{\partial \vec{v}}{\partial z}\right| \ , \qquad (10)$$

where u_* is the local friction velocity. We then propose a prognostic equation for λ based on simple intuitive ideas. In this model, the rate of change of the mixing length is assumed to be

proportional to $(\lambda_s - \lambda)$ where λ is the actual value of the mixing length, and λ_s is the value λ would attain if the boundary conditions (including the geostrophic wind) were kept constant at any given time. Furthermore, the time scale for the change of the size of the energy-containing eddies is assumed to be inversely proportional to the strength of the mixing characterized by the local friction velocity u_* and the convective velocity, w_*, where

$$w_* = \left(\frac{g}{T_o}\,\overline{w'T'}\,h\right)^{1/3} \tag{11}$$

and h is the height of the PBL.

The prognostic equation for λ is then

$$\frac{\partial \lambda}{\partial t} = \frac{\lambda_s - \lambda}{a\lambda/(u_*^2 + w_*^2)^{\frac{1}{2}}} \,. \tag{12}$$

In the work presented here, the constant a is arbitrarily set equal to unity.

In general, λ_s will be a slowly varying function of time and will depend on the past history of the flow field. Here we shall assume that

$$\lambda_s = \frac{kz}{\phi_m}\left(1 - \frac{z}{h}\right) \quad \text{for} \quad z \leq h' \,, \tag{13}$$

$$\lambda_s = \lambda_B \quad \text{for} \quad z > h' \,,$$

where h' ($\sim h$) is the height at which λ_s equals λ_B, a residual mixing length which accounts for the slight mixing above the PBL. When u_* or w_* is relatively large, 0.25 ms^{-1} say, the time scale, $a\lambda/(u_*^2 + w_*^2)^{\frac{1}{2}}$, for eddies of a typical size of 500 m is 2000 s (for a = 1). This time scale is short compared to the characteristic time scale of most dynamical models, and, therefore, it might be appropriate to simply utilize λ_s rather than λ under these conditions. During the transition from an unstable to stable PBL, however, when u_* and w_* may decrease by an order of magnitude, the time scale becomes on the order of several hours. In order to model realistically this transition period, a time-dependent λ may be necessary. Because of the minor increase in computational complexity associated with the prognostic equation for λ, we tentatively retain it pending further sensitivity tests.

The definition (10) of the mixing length is of course somewhat arbitrary and may (as pointed out by J.W. Deardorff in a personal communication) lead to overestimation of the wind shear,

especially in weak wind and strong heating conditions. Under these conditions, it would be more satisfactory to define the mixing length in terms of the turbulent energy, e

$$u^2 \equiv b\lambda e^{\frac{1}{2}} \left|\frac{\partial \vec{v}}{\partial z}\right| \equiv K_m \left|\frac{\partial \vec{v}}{\partial z}\right| \tag{14}$$

where b is a constant and

$$e = \frac{1}{2} \overline{u'_i u'_i} \ .$$

The expression for K_m would then be obtained from the turbulent energy equation, which for horizontal homogeneity may be written in the form

$$\frac{\partial e}{\partial t} = be^{\frac{1}{2}} \lambda \left(\left|\frac{\partial \vec{v}}{\partial z}\right|^2 - \frac{g}{T_o} \frac{K_h}{K_m} \frac{\partial \theta}{\partial z} - A_b \frac{e}{\lambda^2} \right) \tag{15}$$

where we have assumed that the dissipation rate ε may be approximated by

$$\varepsilon = A \frac{e^{3/2}}{\lambda} \tag{16}$$

and that the divergence of the vertical flux of turbulent energy is negligible compared to the other terms.

Neglecting the time-dependent term, $\frac{\partial e}{\partial t}$, and using (14), we obtain

$$K_m = A^{-\frac{1}{2}} b^{3/2} \lambda^2 \left(\left|\frac{\partial \vec{v}}{\partial z}\right|^2 - \frac{g}{T_o} \frac{K_h}{K_m} \frac{\partial \theta}{\partial z} \right)^{\frac{1}{2}} \ . \tag{17}$$

Under neutral conditions, K_m should be given by (10), which implies that $b = A^{1/3}$. For moderate wind conditions and weak heating, the shear term in (17) dominates the convective term and the expression for K_m becomes similar to that given by (10). In the experiment reported here, which involves moderate wind speeds (geostrophic wind = 10 ms^{-1}), K_m is calculated from (10). A comparison experiment utilizing (17) instead of (10) to compute K_m showed similar momentum and potential temperature profiles.

Under the assumption that the stress is in the direction of the shear, the vertical flux-terms are related to the mixing length by

$$-\overline{u'w'} = K_m \frac{\partial u}{\partial z} \tag{18}$$

$$-\overline{v'w'} = K_m \frac{\partial v}{\partial z} \tag{19}$$

$$-\overline{w'T'} = K_h \frac{\partial \theta_c}{\partial z} , \tag{20}$$

where $\frac{\partial \theta_c}{\partial z} = \frac{\partial \theta}{\partial z} - \gamma_c$. The inclusion of γ_c in (20) allows an upward heat flux in weakly stable conditions, and represents the countergradient heat flux (Deardorff, 1966). Deardorff (1966) suggests from theoretical considerations that $\gamma_c \sim 0.7 \times 10^{-3}$ °K m^{-1}. The expression for K_h in (20) is derived from the Kansas experiment (Businger et al., 1971),

$$\frac{K_h}{K_m} = \left(\frac{\phi_m}{\phi_h} \right) = \begin{cases} \dfrac{1.0 + 4.7\ z/L}{0.74 + 4.7\ z/L} & \text{for } z/L > 0 \\ \dfrac{1.35\ (1 - 9\ z/L)^{\frac{1}{2}}}{(1 - 15\ z/L)^{1/4}} & \text{for } z/L < 0 \end{cases} \tag{21}$$

The height, h, of the PBL might be chosen in a number of ways, for example, a fraction of u_*/f under stable conditions or as the height of the capping inversion under unstable conditions. In the present study we use the first height above the ground at which the local Richardson number,

$$Ri = \frac{g}{\theta} \frac{\partial \theta}{\partial z} \Big/ \left| \frac{\partial \vec{v}}{\partial z} \right|^2 \tag{22}$$

exceeds a critical value of 1/4.

c. Initial and boundary conditions

The vertical temperature profile observed at 0835 CST, August 25, 1953 at O'Neill, Nebraska, during the Great Plains Experiment (Stull, 1973) is used to specify the initial conditions for potential temperature. A nearly adiabatic layer is capped with a strong inversion above 400 m (Fig. 6a). The orientation of the model is chosen such that its x-axis points toward the east. The geostrophic wind components are assumed to be $u_g = 10$ m s^{-1} and $v_g = 0$. The initial vertical wind profiles of u and v are obtained by integrating the model for four hours keeping the height of the inversion fixed and without any sur-

face heat flux until a quasi-steady state wind profile is reached. The grid consists of 20 points in the vertical. The first level is located at 0 m, the second at 10 m. Above 10 m, the levels are located every 100 m (at 110, 210, 310 m, etc.). Since the formulation of the heat and momentum fluxes in the PBL and in the surface layer approach each other asymptotically, the choice of the height of the surface layer (10 m in the present model) affects the solution only slightly. The fluxes, mixing length, wind shear and temperature gradients are defined at levels halfway between the levels at which the velocity components and the temperature are computed. At the topmost level, the wind is geostrophic and the temperature is constant. The surface roughness parameter, z_0, is 1 cm, and the mixing length, λ, equals λ_s initially, with λ_s given by (13) and λ_B = 3 m.

The heat flux at the ground is specified by the function

$$\overline{w'T'} = \text{Max} \begin{cases} 0.25 \sin \left(2\pi \ (t - t_o)/24h\right) \\ -0.06 \end{cases} \quad {}^{o}K \text{ m s}^{-1} . \tag{23}$$

The sinusoidal representation of the surface heat flux cycle is limited by -0.06 ^{o}K m s^{-1} after about 12.9 h to simulate crudely the nearly constant heat flux during the night. Sunrise ($t = t_o$) is set at 0635 CST. The maximum heat flux associated with this function is about 18% of the solar constant. Amplitudes of 0.20 and 0.30 ^{o}K m s^{-1} were also tested, but the value of 0.25 ^{o}K m s^{-1} gave the closest agreement between the predicted and the observed heights of the inversion. The value for the negative heat flux is also arbitrary, and was chosen to test the model under stable conditions.

The model was integrated for 24 hours beginning at 0835 CST using a forward-in-time, centered-in-space finite difference scheme. The time step, Δt, was varied from 10 to 60 s, so that the computational criterion, $(\frac{K\Delta t}{\Delta z^2}) < 0.25$ was maintained at every level during the entire integration. Here, K is the maximum of K_m or K_h. The 24 h integration requires about 45 s on an IBM 370/168.

5. Results

a. Time-Height Variation of Mixing Lengths

The time-height variation of the mixing length, λ, is shown in Fig. 1. After two hours of integration (1035 CST) the maximum value of λ has grown from 50 m to 200 m beneath the inversion. The dotted lines show the "stationary" values. As more heat is added, the inversion rises and λ continues to increase below the inversion. In the vertical, λ is proportional to kz near the surface, reaches a minimum at a level which is slightly higher than 1/2 the height of the inversion, and decreases to nearly zero at the inversion. This vertical variation is similar to Blackadar's

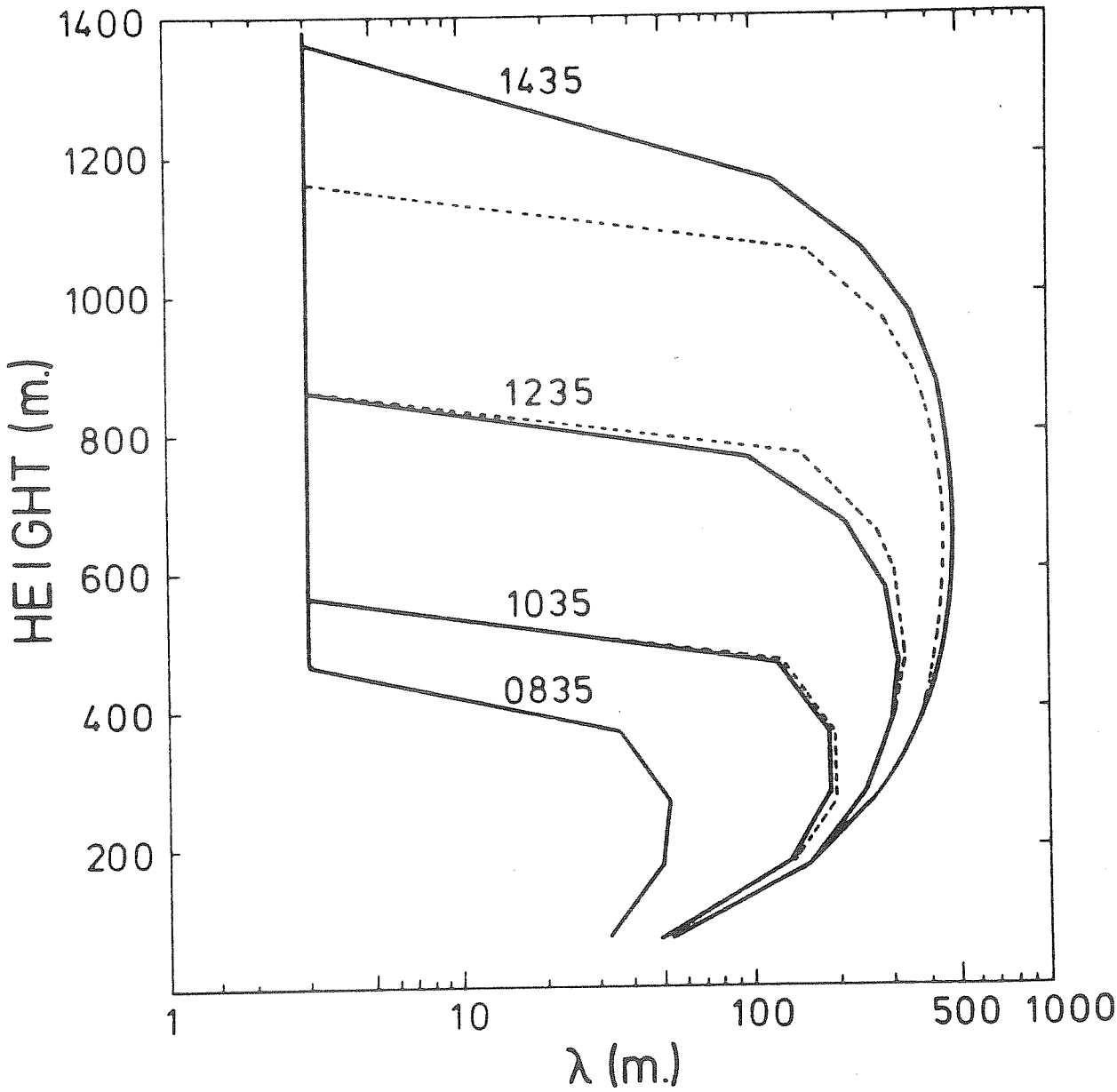

Figure 1 The time variation of mixing length, λ, under unstable conditions. The dashed lines denote values of λ_s.

(1962) and Shir's (1973) results for the neutral PBL. However, because λ in this model depends on the upward heat flux through (12), the magnitudes here are much larger than Blackadar's and Shir's values, reaching about 1/3 of the height of the inversion.

The time scale of λ in (12) is inversely proportional to the local stress. Near the ground, where the stress is large, λ approaches its stationary value rapidly. In the upper part of the PBL, where the local stress is less, λ responds more slowly. Also, the stationary value of the mixing length, λ_s, is changing at this level in response to the rising inversion height (eq. 13).

After 1835 CST the surface heat flux becomes negative and the turbulence in the PBL begins to decay, as shown by the decrease of λ in Fig. 2. Because of the reduced values of stress, the mixing length changes at a slower rate during the night than during the day. Near the surface, λ adjusts to the stationary value in 1-2 hours, while in the upper portion of the PBL the adjustment requires 3-4 hours. As shown in Fig. 1, the time-dependent mixing length is very close to the stationary value under unstable conditions, which indicates that the use of the prognostic equation for λ during these conditions is unnecessary. However, under stable conditions (Fig. 2), the actual mixing length differs by an order of magnitude from the stationary value, indicating that a prognostic equation for the mixing length (Eq. 12) is important in this parameterization of the stable PBL.

The vertical diffusivity for momentum, K_m, is plotted in Fig. 3. The vertical profiles of K_m resemble those proposed by O'Brien (1970) and Agee et al. (1973). Here, K_m not only varies with the height of the inversion but also changes with the wind shear and stability in the PBL. The profiles show a nearly linear increase of K_m near the ground, a maximum value near 1/3 of the height of PBL, and a rapid decrease near the inversion. The maximum value of K_m varies by an order of magnitude as the PBL changes from neutral to unstable.

b. Vertical Profiles of Stresses and Heat Flux

The profile of total stress is shown in Fig. 4. Both Deardorff's (1974) three-dimensional simulations and Wyngaard and Cote's (1974) results from a second-order closure scheme indicate that the stresses in the boundary layer vary linearly with height. The stress shown in Fig. 4 is nearly linear, but concave slightly upward, in agreement with Shir's (1973) results for a neutral boundary layer.

The heat flux profiles shown in Fig. 5, are very close to the idealized profile given by Stull (1973, p. 1093). Below the inversion, the heat flux is a linear function of height. A downward heat flux occurs at the inversion. This heat flux profile produces a rising inversion with time (Fig. 6b). The magnitude of the downward heat flux is about 10% of the surface heat flux, which is the correct order of magnitude (Lilly, 1968; Wyngaard and Cote, 1974). The behavior of the downward heat flux in this model represents an improvement over simpler K-theory models

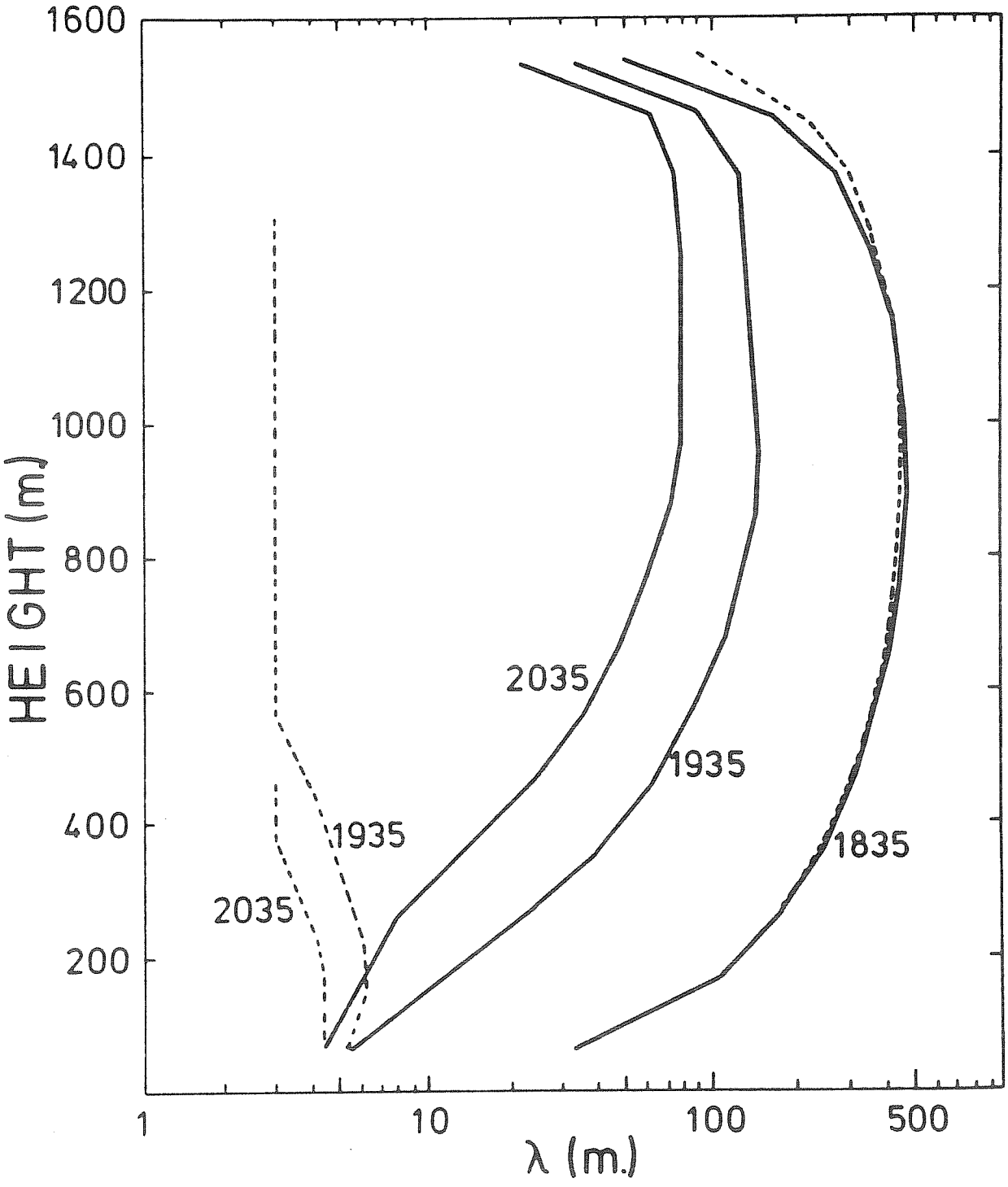

Figure 2 The time variation of mixing length, λ, under stable conditions. The dashed lines denote values of λ_s.

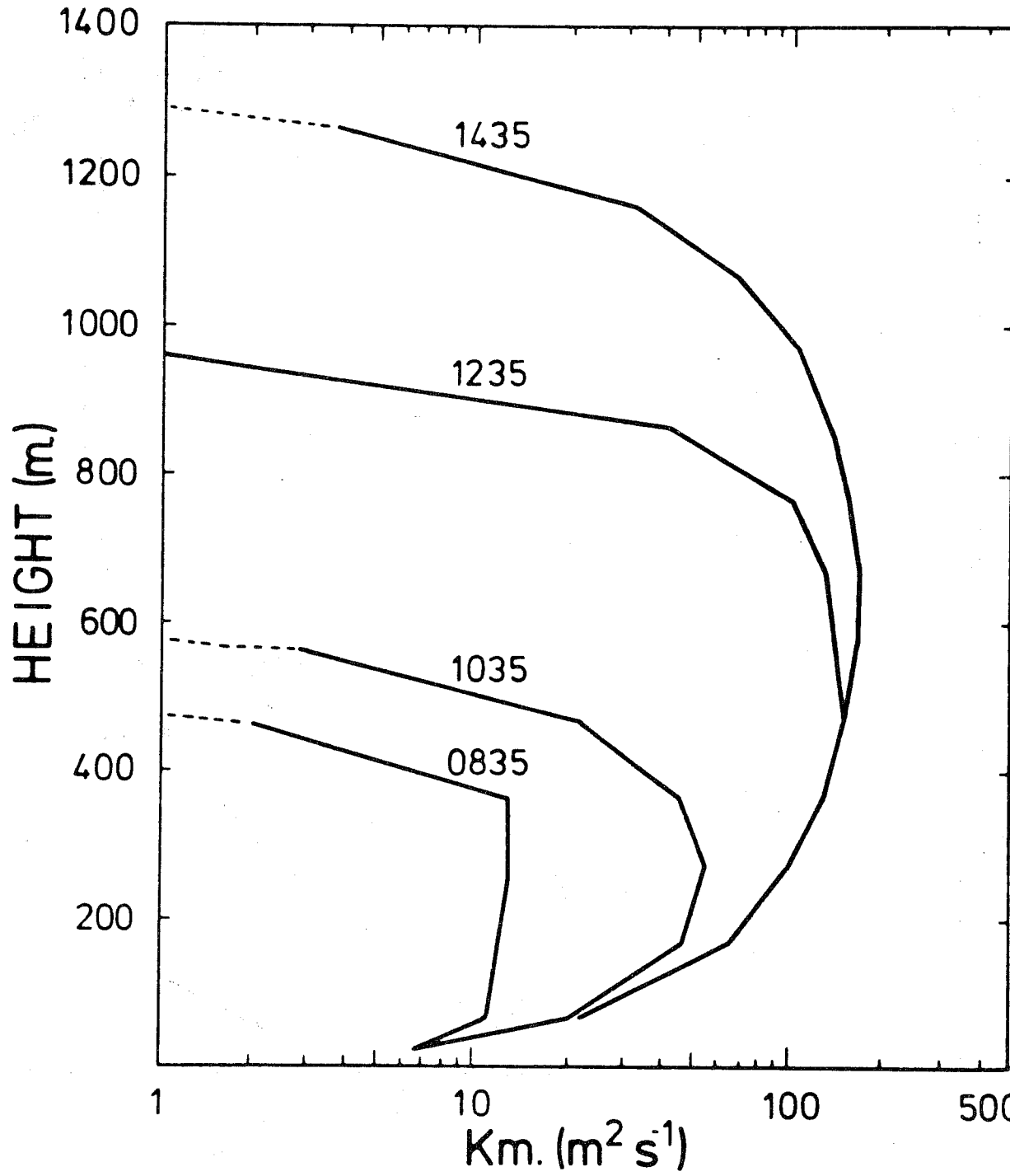

Figure 3 The time variation of the kinematic coefficient of eddy viscosity for momentum K_m.

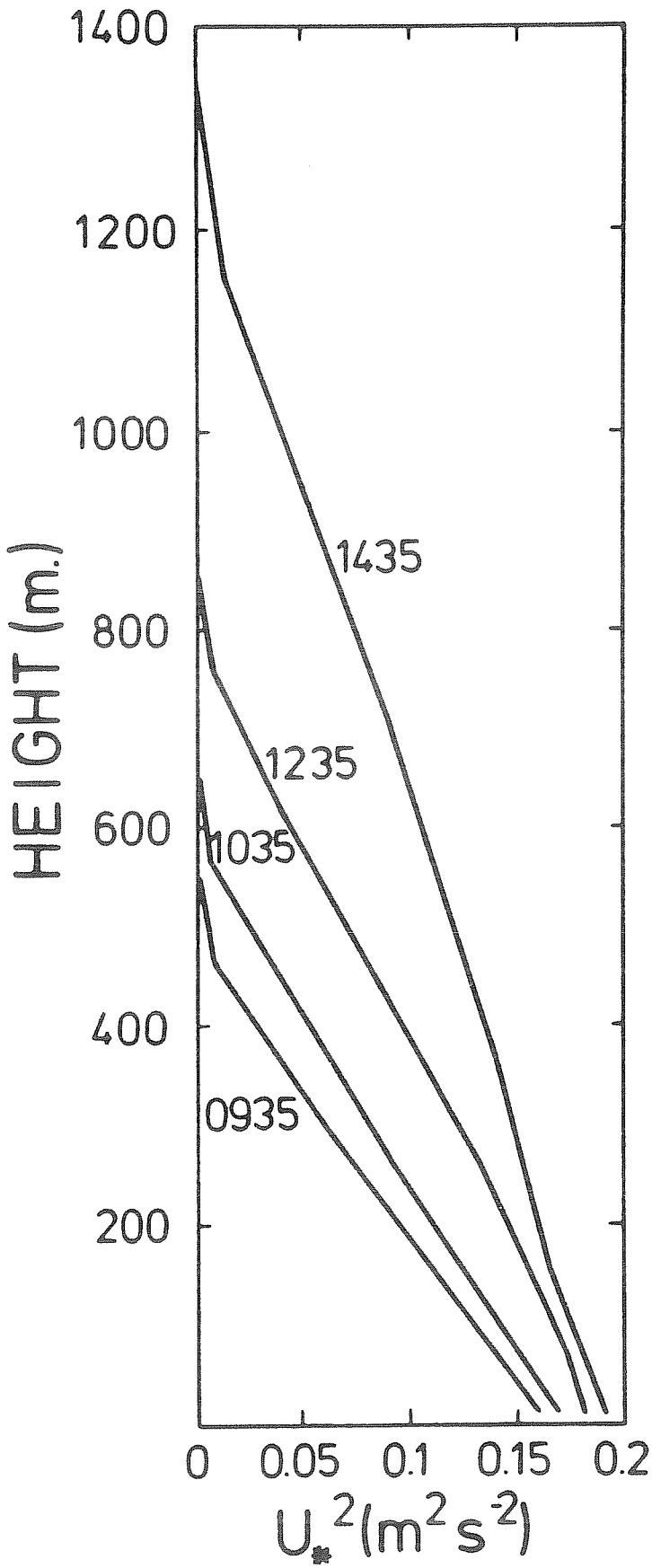

Figure 4 The time variation of the vertical profiles of u_*^2 under unstable conditions.

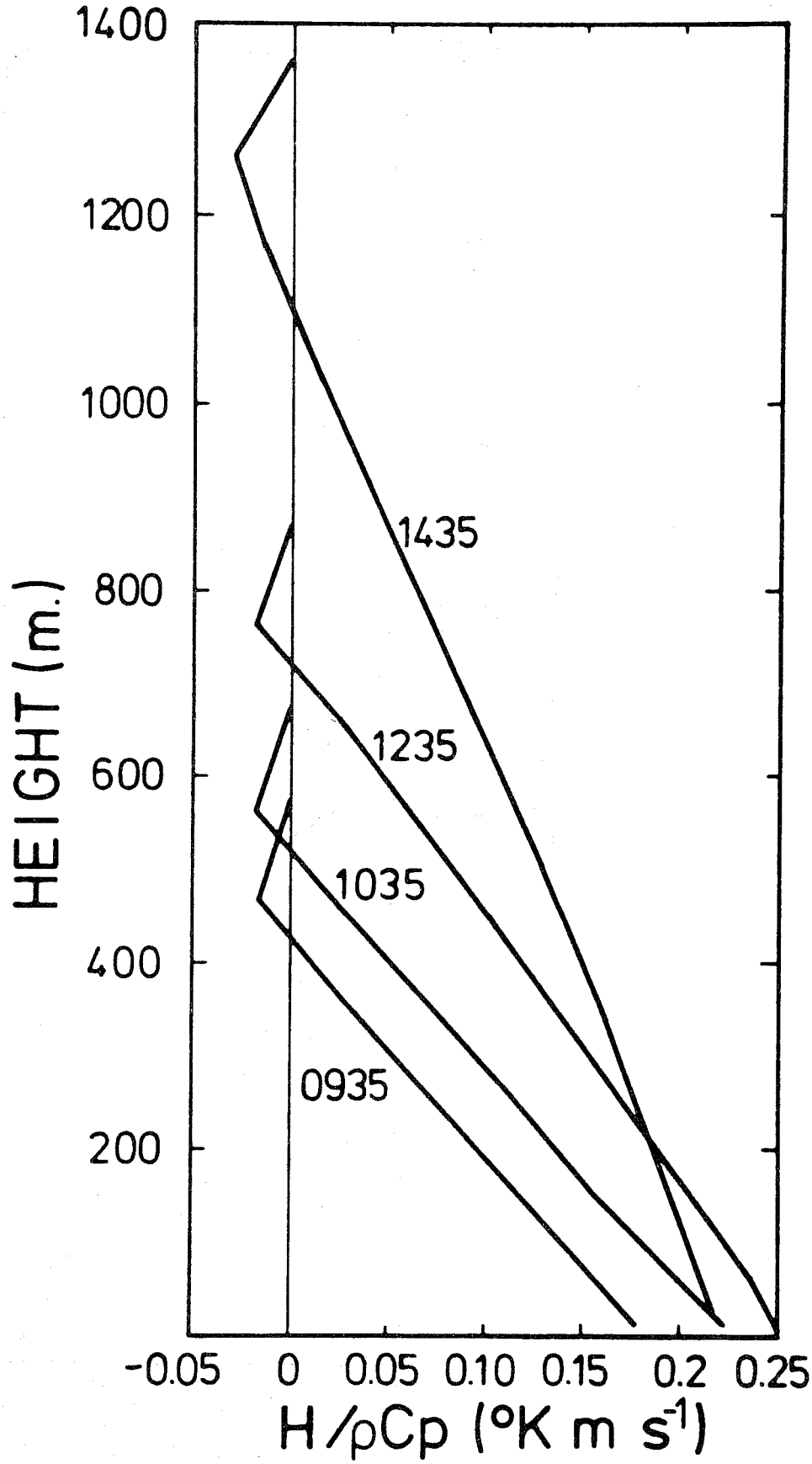

Figure 5 The time variation of the vertical profiles of heat flux under unstable conditions.

which produce a larger downward heat flux above the inversion and an unrealistically large cooling above the inversion.

c. The Rise of the Inversion

The observed time variation of the inversion during the Great Plains Experiment (Stull, 1973) is shown in Fig. 6a and the variation predicted by the model is shown in Fig. 6b. The model reproduces the rising inversion, a slightly stable lapse rate below the inversion and a slightly superadiabatic lapse rate near the ground. Minor differences in the predicted and observed profile may be attributed to the arbitrarily specified surface heat flux, the arbitrary initial conditions for λ and the neglect of other physical processes such as radiation, horizontal advection, and synoptic-scale vertical motions.

d. Behavior of the Stable PBL

After 18:35 CST, the specified heating function becomes negative. The magnitude of the downward heat flux and the associated low-level cooling may not be realistic because radiation is neglected. It is mainly the long wave radiation, not the sensible heat flux divergence that is responsible for the nocturnal cooling. However, the arbitrary specification of cooling should be sufficient to illustrate the time-dependent behavior of the PBL under stable conditions.

Figure 7 shows that potential temperature profile at 18:35, 20:35 and 22:35 CST. An inversion forms near the ground as the height of the upper inversion decreases slowly. The heat flux is downward below and weakly positive above the lower inversion.

During the day when the vertical mixing is strong, the directional wind shear is small, averaging only $2\text{-}3^{o}$ over 400 m (see Fig. 8). As the PBL becomes stable, the winds adjust to the pressure gradient force and the decreased frictional force. In Fig. 8, the wind above 410 m veers toward the geostrophic wind direction when the downward momentum transfer is reduced. The wind below 410 m, deprived of downward momentum transfer from higher levels, backs toward a larger cross-isobar flow angle. Figure 8 also shows a rapid change of wind direction at lower levels and a more delayed response at higher levels.

Figure 9 shows the formation of a nocturnal low-level jet in the stable PBL (Blackadar, 1957). The jet is mainly confined below 400 m where the wind direction first backs due to reduced mixing then veers (after 2300 CST) due to Coriolis forcing. However, the wind in the surface layer decreases considerably during the formation of the nocturnal jet. Figure 10 illustrates the wind speeds at 10, 110 and 410 m. The wind at anemometer level decreases by 4 m s^{-1} in the stable PBL, while the wind at 210 m increases by 2-3 m s^{-1}. Recently Goff and Duchon (1974) presented results from over half a year's observation from a 444 m tower. Although their results contain synoptic-scale variations, the diurnal variation in wind predicted by this model is similar to

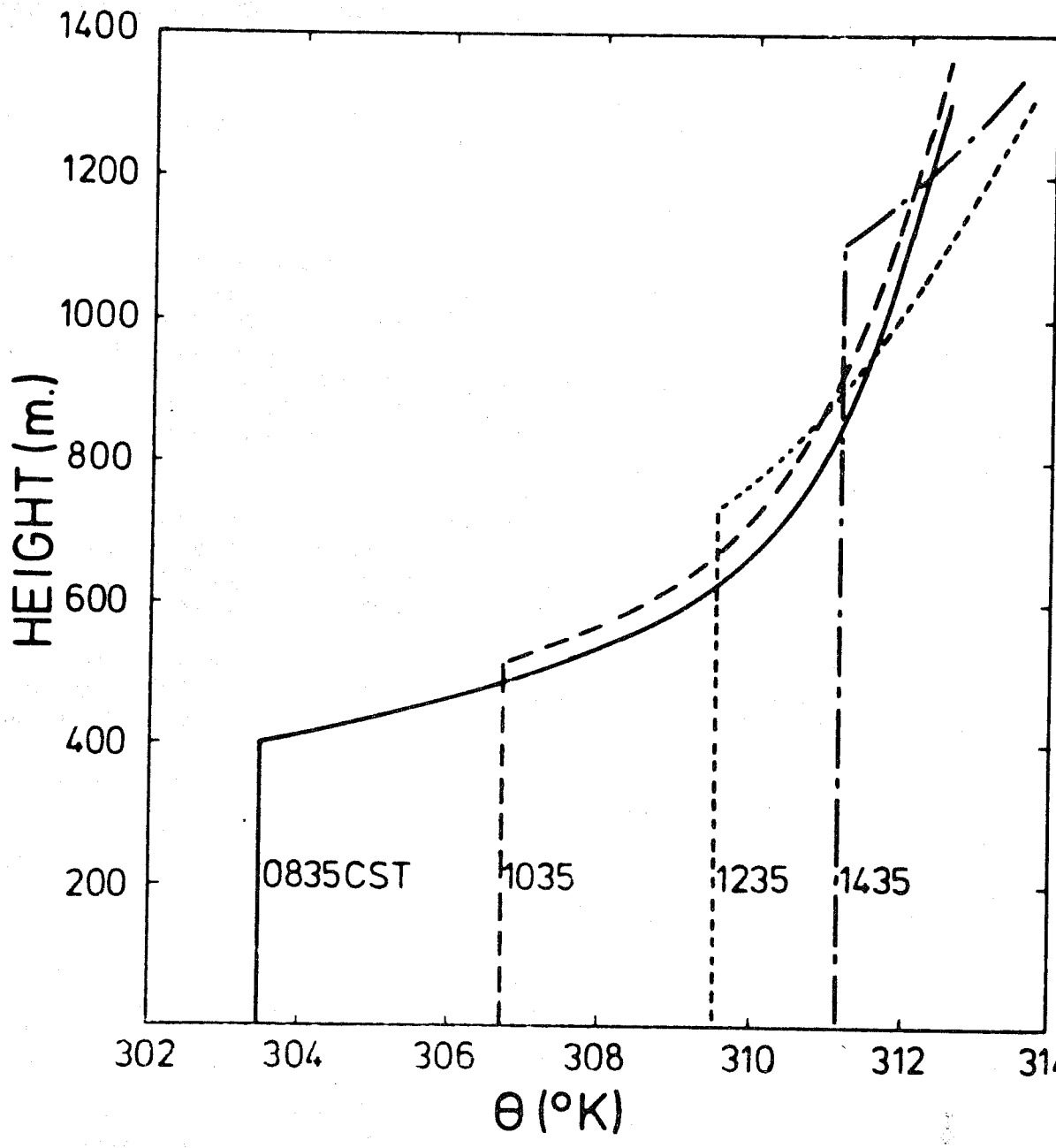

Figure 6a Observed vertical profiles of potential temperature during the Great Plains Experiment (Stull, 1973).

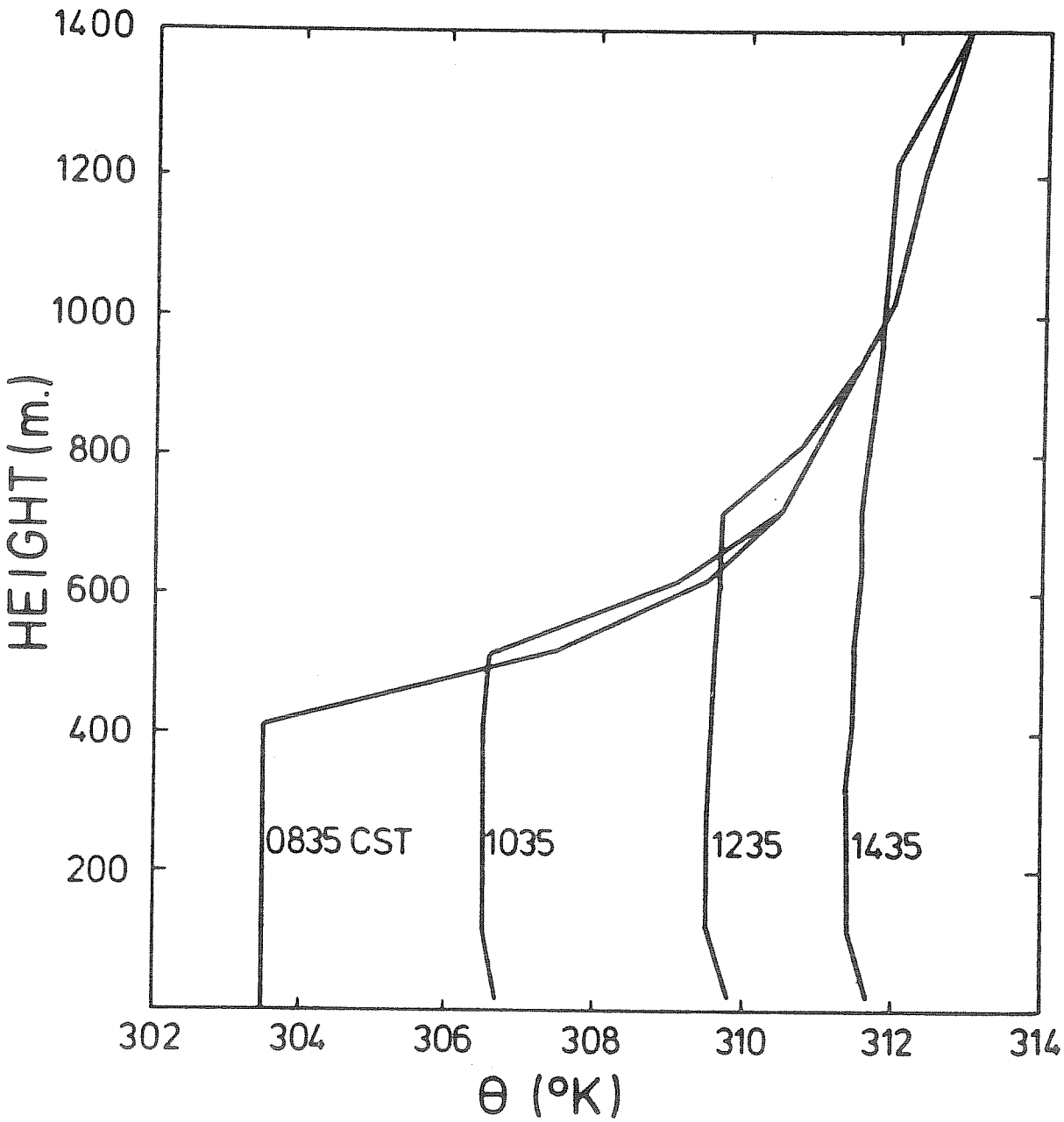

Figure 6b Predicted vertical profiles of potential temperature under unstable conditions.

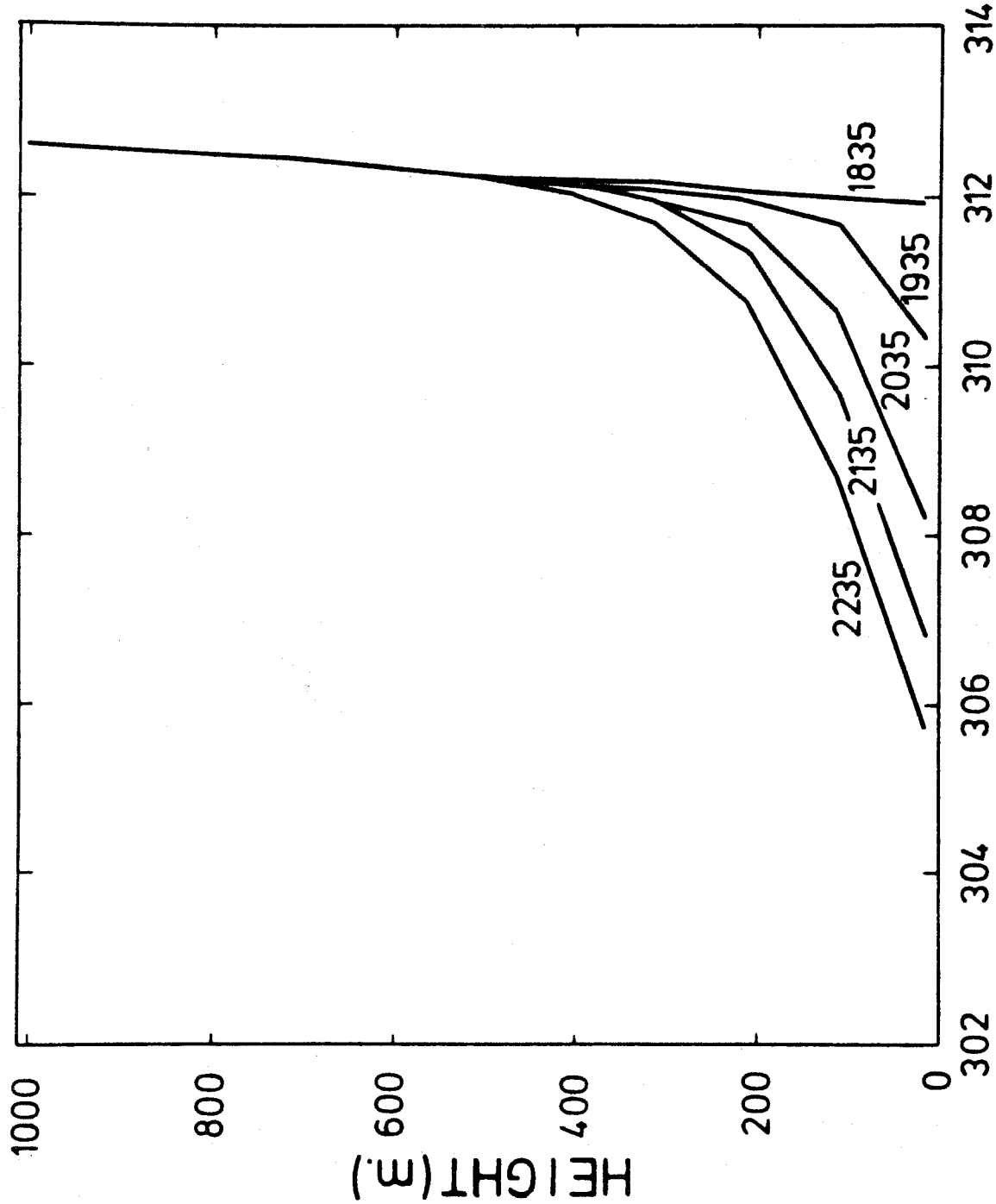

Figure 7 Predicted vertical profile of potential temperature field under stable conditions.

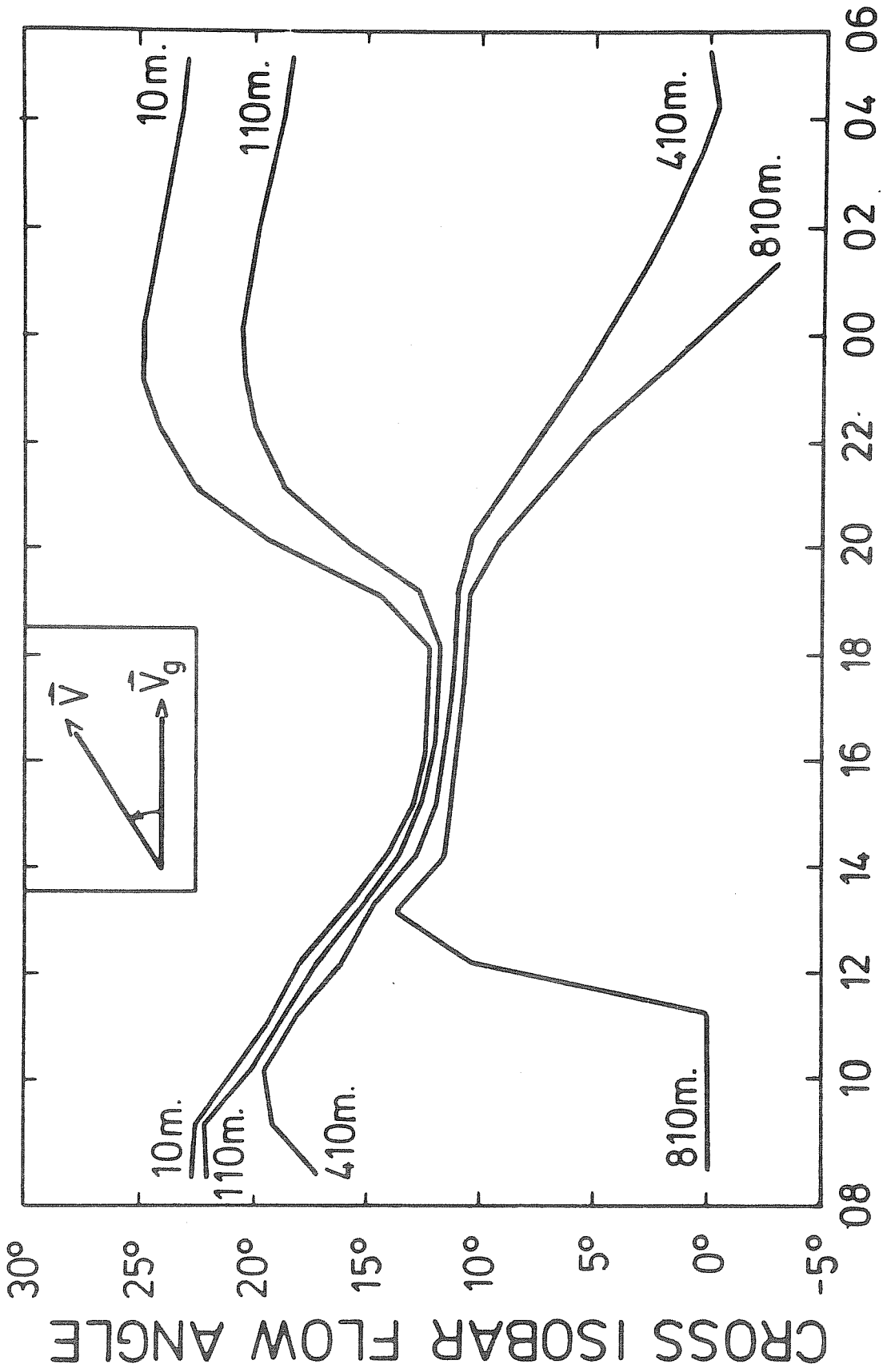

Figure 8 The time variation of the cross-isobaric flow angle at 10, 110, 410 and 810 m.

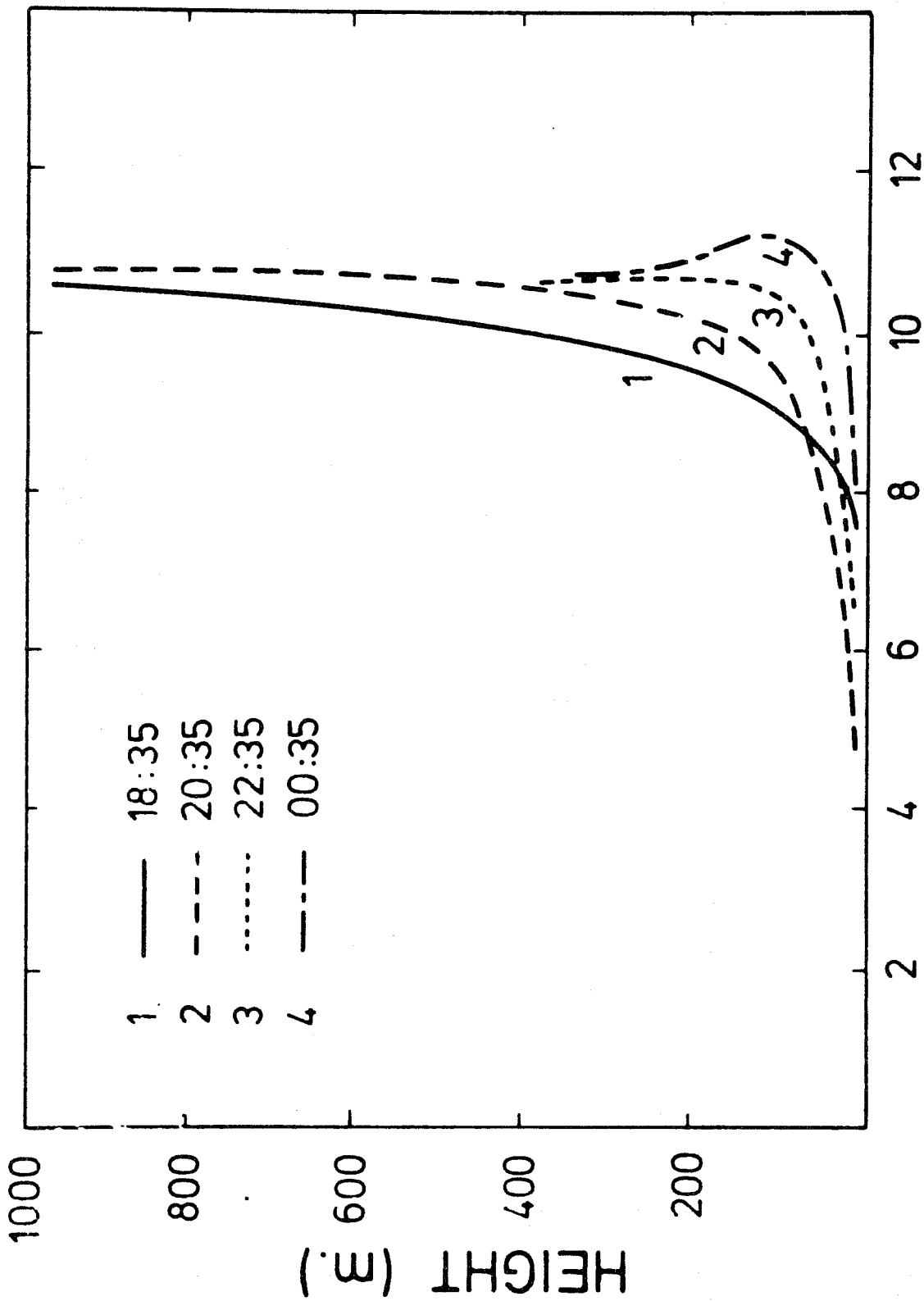

Figure 9 Vertical profiles of the wind speed showing the formation of a nocturnal low-level jet.

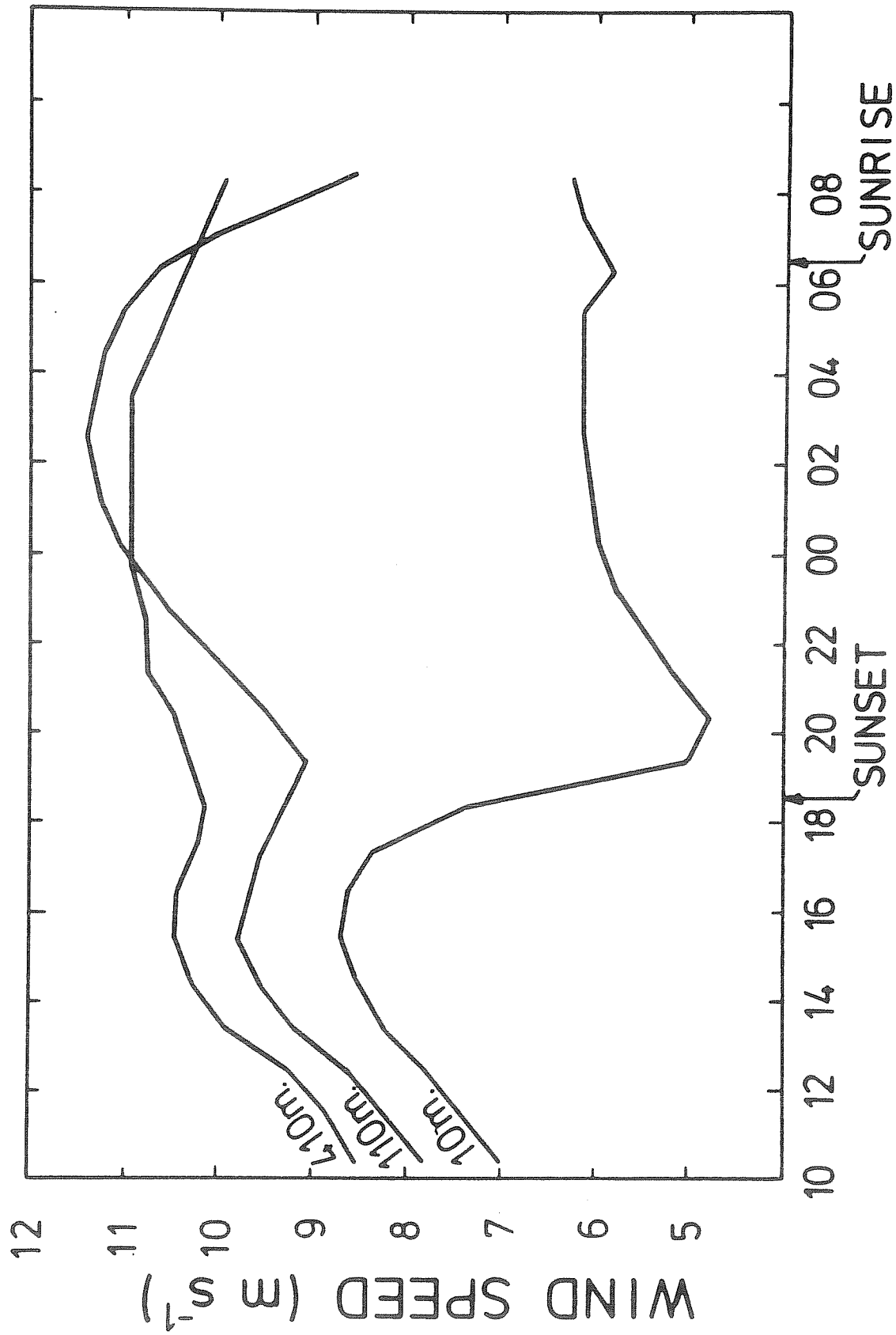

Figure 10 The time variation of wind speed at heights of 10, 110 and 410 m.

the observed diurnal variations of mean wind speed.

e. Vertical Diffusion of a Passive Substance

In this section the model is utilized to predict the vertical diffusion of a passive substance, q, which is governed by the equation,

$$\frac{\partial q}{\partial t} = -\frac{1}{\rho}\frac{\partial \rho \overline{w'q'}}{\partial z} , \tag{24}$$

where

$$\overline{w'q'} = -(\phi_m/\phi_h)\lambda^2 \left|\frac{\partial \vec{v}}{\partial z}\right| \frac{\partial q}{\partial z} . \tag{25}$$

Figure 11 shows the concentration of a passive substance, q, when the flux of q is constant at the ground. This experiment simulates the diffusion of a pollutant from a site with a constant rate of emission. The concentration during the "day" stays nearly constant below the inversion as the substance diffuses upward following the rising of the inversion. The upward flux is limited by the height of the inversion, and a sharp vertical gradient of q is maintained at the inversion level at all times. After "sunset", when the surface heat flux becomes negative, the low-level concentration increases rapidly under the newly formed inversion, while the concentration in the upper parts of PBL remains unchanged. It is often observed in the early morning that the polluted layer over the urban area is much thicker than the height of the lowest inversion. This pollution had been mixed upward during the previous day.

Of course, in order to predict urban pollution, horizontal inhomogeneities are important and advection must be included in the model. However, this simple vertical diffusion model appears to calculate the vertical turbulent fluxes in a realistic way, and hence to have the potential for incorporation into mesoscale dynamic models.

6. Summary

Although second-order closure schemes have considerable theoretical appeal, they are time consuming. Therefore, when it is necessary to describe the PBL in some detail for the purposes of resolving important interactions of the PBL with a coupled dynamic model, simpler first-order closure schemes (K-theories) still have an important role to play. In this paper a simple model of the PBL is proposed. The surface layer is modeled according to established similarity theory. Above the surface layer, a time-dependent mixing length is utilized which is a function of the

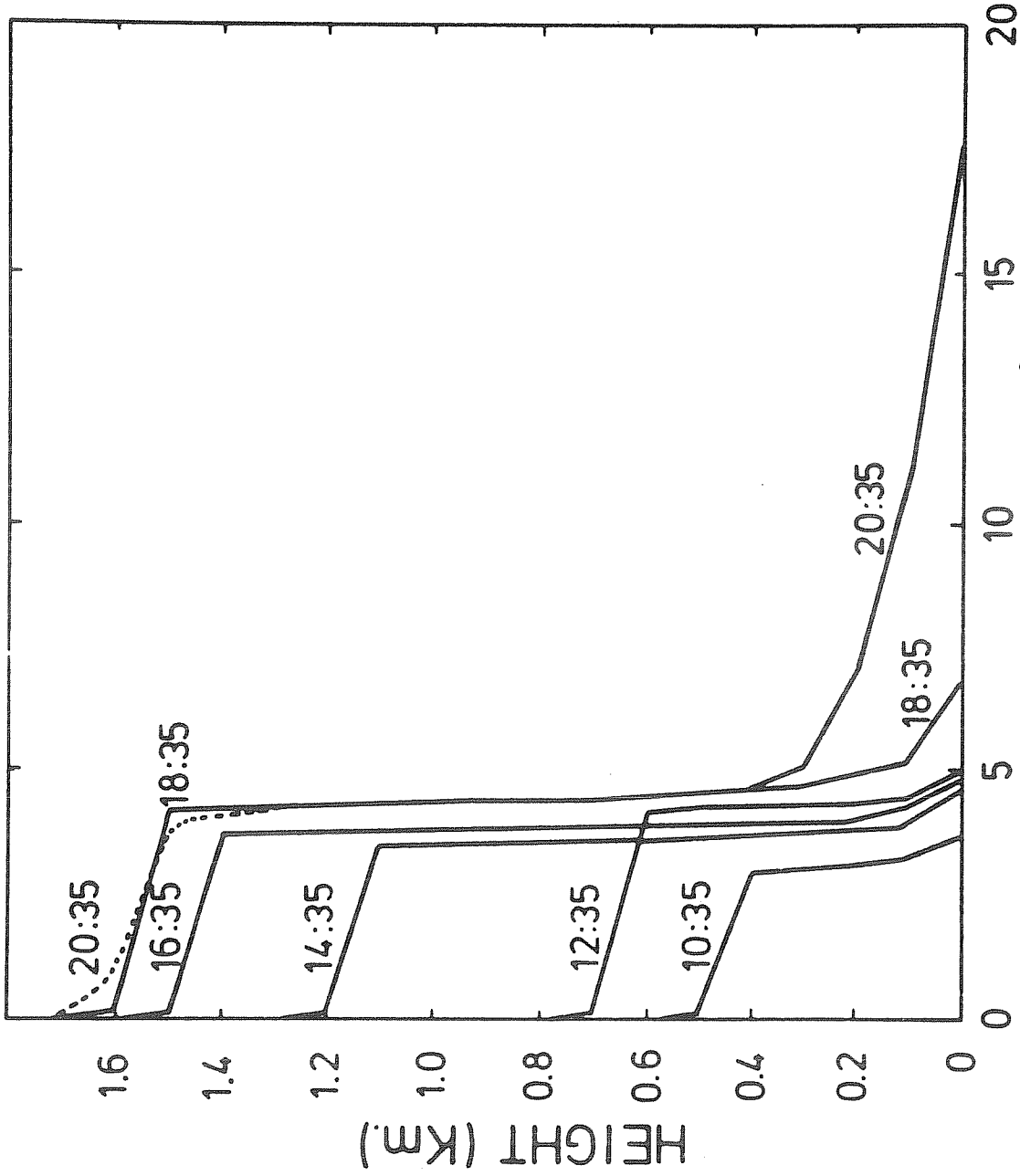

Figure 11 The time variation of concentration of q in the PBL when the upward flux of q is kept constant at the surface.

PBL characteristics, including the height of the capping inversion as well as the surface heat flux. In a preliminary experiment, the behavior of the PBL agrees well with the observations of the Great Plains Experiment.

Acknowledgments

This work was supported by The Environmental Protection Agency Grant GR800397.

References

Agee, E.M., D.E. Brown, T.S. Chen and K.E. Dowell, 1973: A height-dependent model of eddy viscosity in the planetary boundary layer. J. Atmos. Sci., 30, 409-412.

Anthes, R.A., 1972: The development of asymmetries in a three-dimensional numerical model of the tropical cyclone. Mon. Wea. Rev., 100(6), 461-476.

Blackadar, A.K., 1957: Boundary layer wind maxima and their significance for the growth of nocturnal inversions. Bulletin of the American Meteorological Society, 38, 283-290.

Blackadar, A.K., 1962: The vertical distribution of wind and turbulent exchange in a neutral atmosphere. J. Geophys. Res., 67, 3095-3102.

Businger, J.A., 1973: Workshop on Micrometeorology. American Meteorological Society. 67-98.

Businger, J.A., J.C. Wyngaard, Y. Izumi and E.F. Bradley, 1971: Flux-profile relationship in the atmospheric surface layer. J. Atmos. Sci., 28, 181-189.

Clarke, R.H., 1970: Recommended methods for the treatment of the boundary layer in numerical models. Australian Meteorological Magazine, 18(2), 51-71.

Deardorff, J.W., 1966: The countergradient heat flux in the lower atmosphere and in the laboratory. J. Atmos. Sci., 23, 503-506.

Deardorff, J.W., 1972a: Numerical investigation of neutral and unstable planetary boundary layers. J. Atmos. Sci., 11(1), 91-115.

Deardorff, J.W., 1972b: Parameterization of the planetary boundary layer for use in general circulation models. Mon. Wea. Rev., 100(2), 93-106.

Deardorff, J.W., 1974: Three-dimensional numerical study of the height and mean structure of a heated planetary boundary layer. Boundary Layer Meteorology, 7, 81-106.

Donaldson, C. dup., 1973: Workshop on Micrometeorology. American Meteorological Society, 313-390.

Estoque, M.A., 1973: Workshop on Micrometeorology. American Meteorological Society. 217-268.

Goff, R.C. and C.E. Duchon, 1974: Low-frequency temperature spectra from a 444 meter tower. J. Atmos. Sci., 31, 1164-1166.

Lilly, D.K., 1968: Model of cloud-topped mixed layers under a strong inversion. Quart. J. Roy. Meteo. Soc., 94, 292-309.

Lumley, J.L. and B. Khajeh-Nouri, 1974: Computational modeling of turbulent transport. Advances in Geophysics. 18A, 169-192.

O'Brian, J.J., 1970: A note on the vertical structure of the eddy exchange coefficient in the planetary boundary layer. J. Atmos. Sci., 27, 1213-1215.

Ooyama, K., 1969: Numerical simulation of the life-cycle of tropical cyclone. J. Atmos. Sci., 26, 3-40.

Panofsky, H.A., 1973: Workshop on Micrometeorology. American Meteorological Society. 151-174.

Rosenthal, S.L., 1970: A circulary symmetric primitive equation model of tropical cyclone development containing an explicit water vapor cycle. Mon. Wea. Rev. 98(9), 643-663.

Sheets, R.C., 1969: Some mean hurricane soundings. J. Appl. Meteor. 8, 134-146.

Shir, C.C., 1973: A preliminary numerical study of atmospheric turbulent flows in the idealized planetary boundary layer. J. Atmos. Sci., 30, 1327-1339.

Stull, R.B., 1973: Inversion rise model based on penetrative convection. J. Atmos. Sci., 30, 1092-1099.

Wyngaard, J.C., O.R. Cote and K.S. Rao., 1974: Modeling the atmospheric boundary layer. Advances in Geophysics., 18A, 193-211. Academic Press, Inc., New York, New York.

Wyngaard, J.C. and O.R. Cote, 1974: The evolution of a convective planetary boundary layer model - a high-order-closure model study. Boundary Layer Meteorology, 7, 289-308.

A P P E N D I X

APPLICATION OF A MULTI-LEVEL PLANETARY BOUNDARY LAYER MODEL TO A HURRICANE MODEL

I. The Hurricane Model

The planetary boundary layer (PBL) parameterization of Busch et al. (1976) is incorporated into an axisymmetric hurricane model. The basic equations are identical to those in Anthes (1971) with the radius and sigma as the two spatial coordinates. Kuo's (1974) modified cumulus parameterization, in which the latent heat released by the convective cumulus clouds is parameterized based on the boundary layer water vapor convergence and the environment conditional instability, is used. The horizontal resolution is 60 km from radius 0 to 1000 km; the grid size is then stretched from radii 1000 km to 3000 km so that the influence of the lateral boundary conditions is reduced to minimum. There are 9 layers in the vertical with 5 layers in the lowest 1 km. Since the basic equations are written in momentum flux form, the mass and momentum data points are staggered in the horizontal in order that the finite differencing forms conserve momentum and mass. The prognostic and the diagnostic quantities are also staggered in the vertical to avoid loss of accuracy through interpolations.

The model is initialized with a weak vortex and a weak warm core. The initial momentum field is in gradient balance with the mass field. Then, the model is integrated by center in time scheme. Before the model storm reaches steady state at 96 h, it experiences an initial filling stage due to friction and horizontal diffusion in the first 24 h, and a fast deepening stage owing to the organized convections between 48 ~ 72 h.

II. The Steady-State Solution and the PBL Characteristics

Figs. 1 and 2 show the steady-state solution of the radial and tangential velocities, respectively. The inflow, as well as the subgradient tangential flow, is confined in the PBL. Very large wind shear is found at the top of the PBL where the maximum wind speed is reached. The vertical velocity field (Fig. 3) shows a strong and rather concentrated "eye wall" convective region. The downward motion prevails in most of the model domain outside the concentrated convection area.

The relative humidity field (Fig. 4) shows high relative humidities in the PBL and the outflow skirt, a rather humid convective core, and a very dry region in the downdraft area. There is a sharp humidity gradient across the PBL top. Since the vertical mixing in the PBL tends to homogenize the mixing ratio and the potential temperature, the relative humidity increases with height in the PBL.

As shown by the temperature anomalies in Fig. 5, the temperature in the PBL is nearly isothermal on a horizontal plane and nearly in equilibrium with the ocean surface temperature. The maximum temperature anomaly is found in the convective core below the tropopause as the strong convective heating there stabilizes the core region. This high anomaly is extended outward as advected by the outflow. The secondary maximum in the

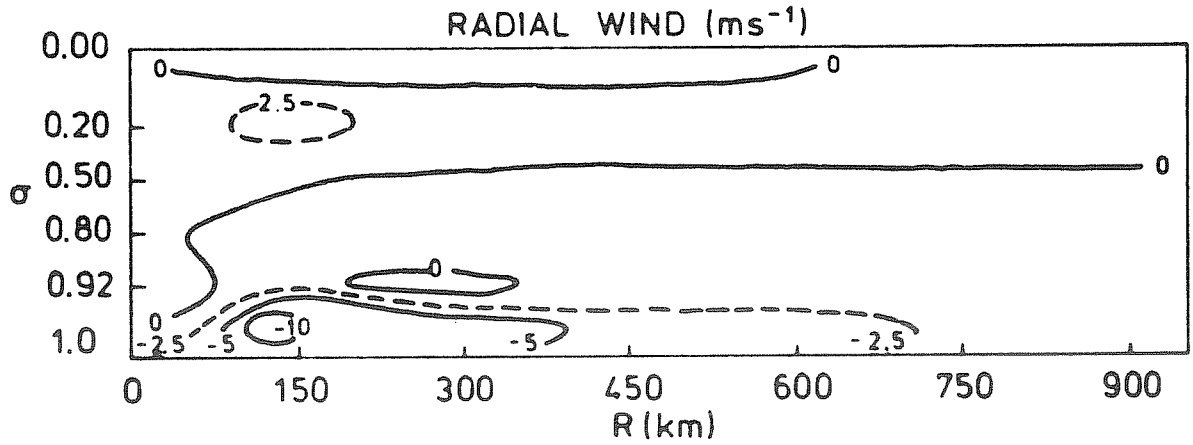

Figure 1 The radial velocity at steady state.

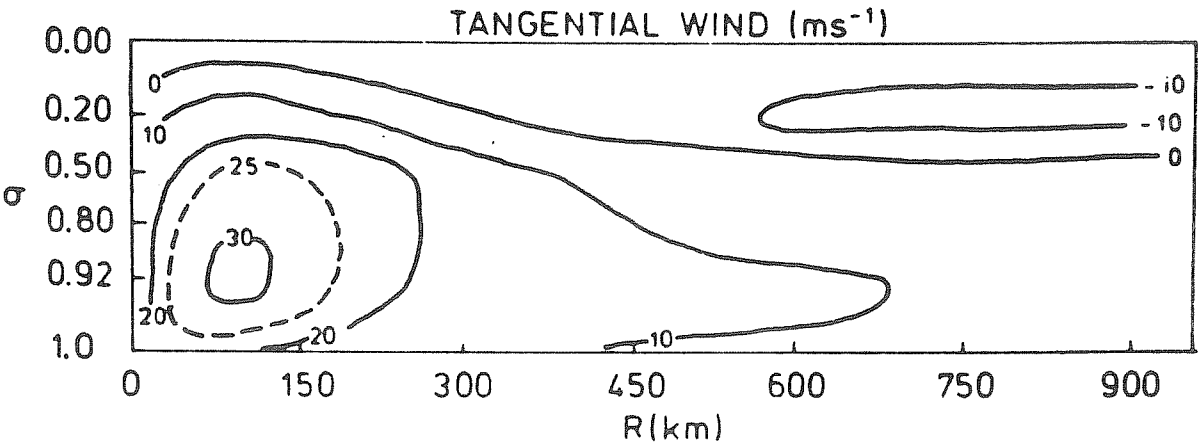

Figure 2 The tangential velocity at steady state.

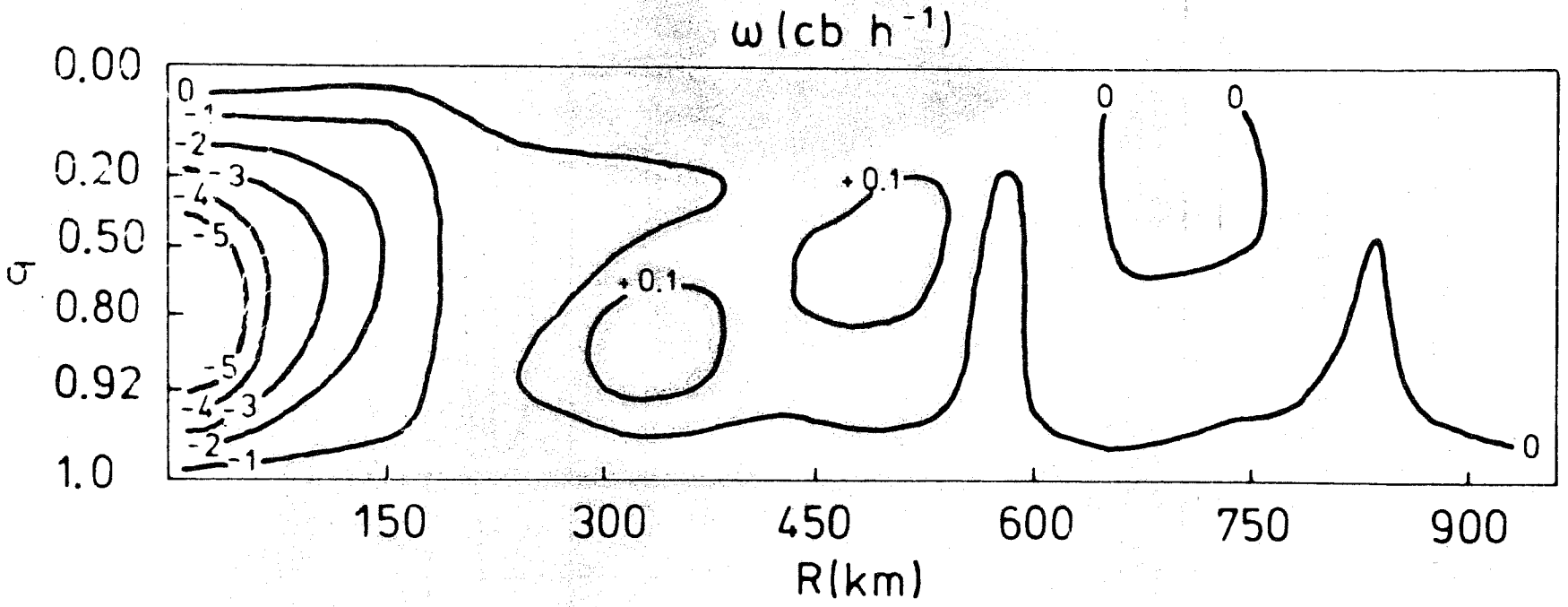

Figure 3 The vertical velocity, $\omega = dp/dt$, at steady state.

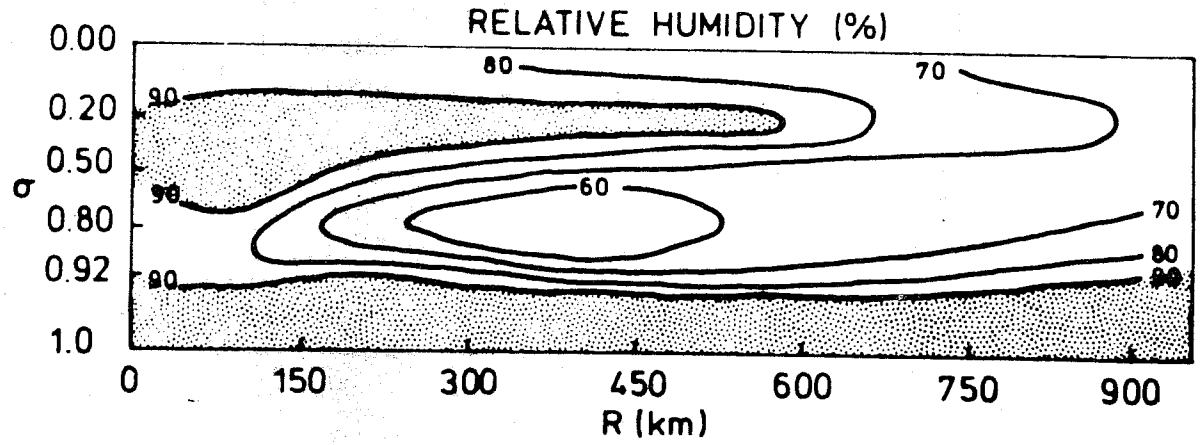

Figure 4 The relative humidity at steady state.

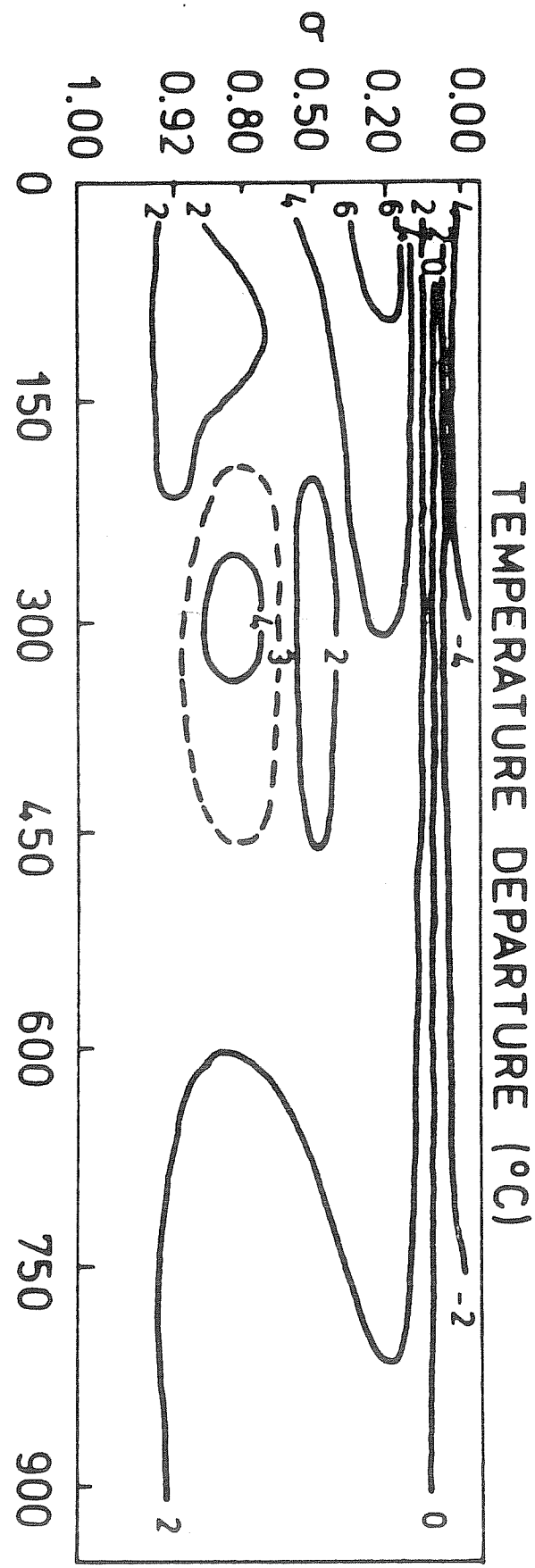

Figure 5 The temperature anomaly (departure from initial boundary conditions) at steady state.

downdraft region is caused by adiabatic heating, while the temperature in the lower part of the convective area remains unchanged due to the fact that the diabatic heating is balanced by the associated ascending motion.

The height of PBL, defined by an abrupt change of potential temperature lapse rate as compared to those in the PBL, is shown in Fig. 6. The height of the PBL is noticeably lifted by the convection near the storm center. It decreases with increasing radius in the downdraft region, reaching a minimum of 350 m near r = 390 km. The height is considerably lower than those in other hurricane models (e.g. Ooyoma, 1968; Anthes et al., 1971) where the height of PBL is approximately 1 km by ad hoc assumptions. Recently, Rosenthal and Moss (1975), based on the observational data, conclude that the PBL in hurricane reaches only 700 m. In addition, the height of the PBL is found to be 600 m in undisturbed area and 400 m in disturbed area in BOMEX data (Nitta, 1975). It is suggested that the growth of the mixed layer is hampered by the cumulus convection. Sarachik (1974) further argues that the tropical mixing layer may be as low as 400 m based on a budget study. Therefore, we consider the height of PBL in this present hurricane model is not unreasonable, though there is no known direct observation in the hurricane to substantiate it.

The vertical diffusion coefficients, K_m and K_H, are shown in Fig. 7. The coefficients increase with height from surface, reaching maxima in the PBL and decreasing toward the top of the PBL. The coefficients are larger in the convective area as a result of strong wind and wind shear. The Richardson number is generally less than critical in most part of the PBL (Fig. 8). The inflow angle (Fig. 9) shows a maximum of 25° outside of the maximum inflow. Compared to the sharp wind direction change at the top of the PBL, the inflow angles in the PBL are rather uniform.

The PBL in the steady-state storm is nearly in thermal equilibrium with the ocean surface, the heat flux is weak and the heating rate is not significant. The heat budget study shows the total vertical eddy heat flux inside the radius of 300 km is slightly negative. Presumably, the heat is entrained downward from the secondary maximum of the temperature anomaly at the downdraft region into the PBL and then advected by the radial velocity. Figs. 10 and 11 show the momentum flux and water vapor flux at various radii. The stress profiles feature linear variations of the tangential stress and curved cariations of the radial stress. The curvature of the radial stress achieves its maximum at small radii where acceleration by horizontal advection is strongest. The water vapor flux is characterized by a nearly constant flux in the PBL and a sudden decrease at the PBL top. The equivalent drag coefficients for momentum and for vapor (Fig. 12) shows high values for high surface wind and the ratio of $C_D/C_q \sim 0.3$.

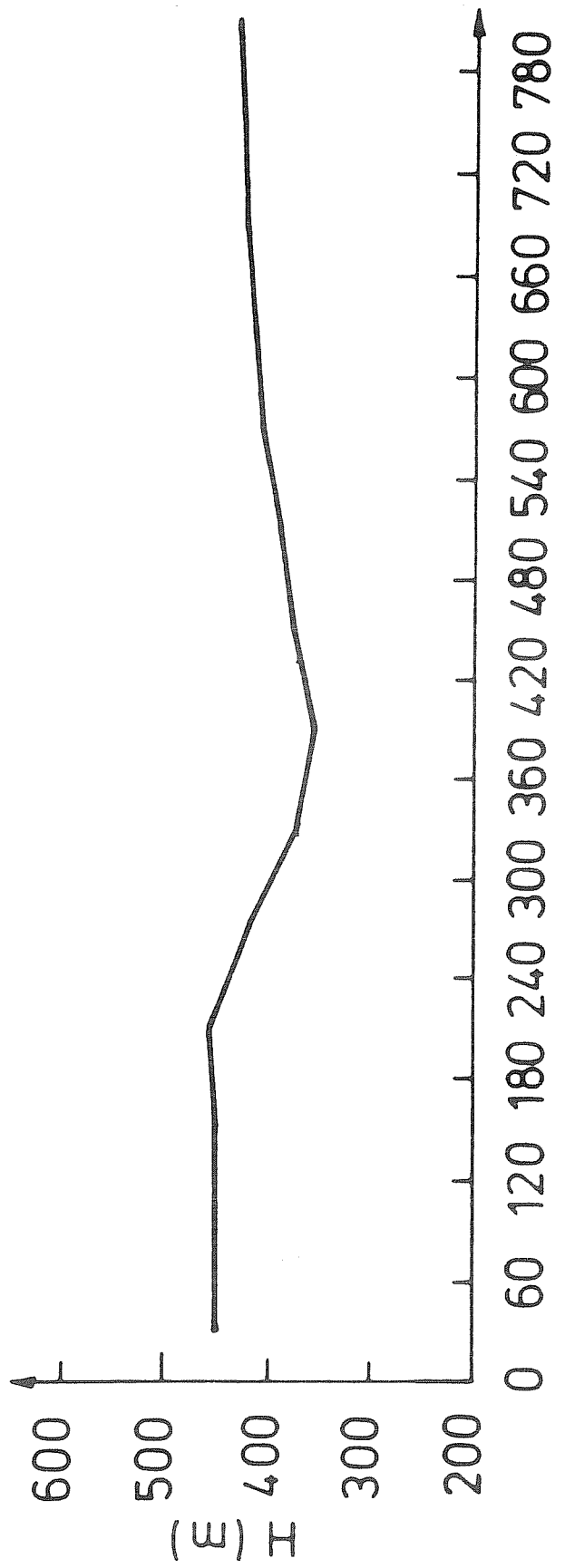

Figure 6 The height of the PBL in the steady state hurricane.

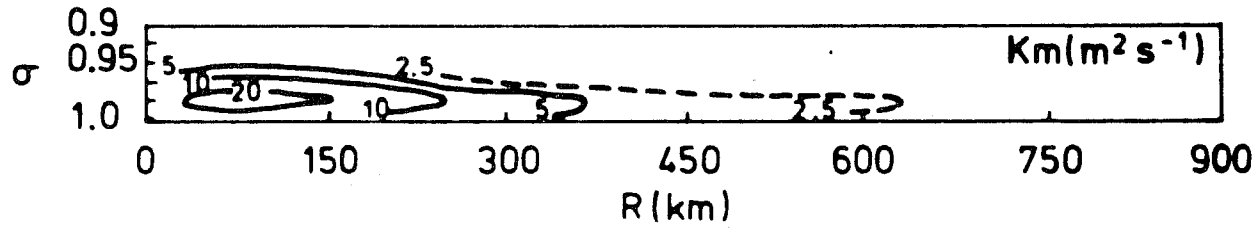

Figure 7a Diffusivity for momentum at steady state.

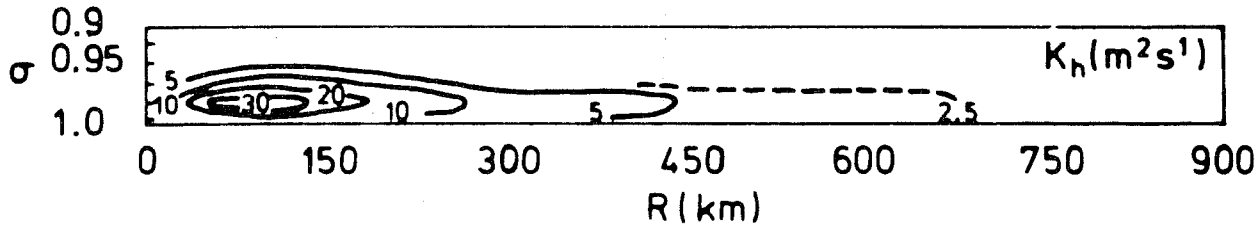

Figure 7b Diffusivity for sensible heat at steady state.

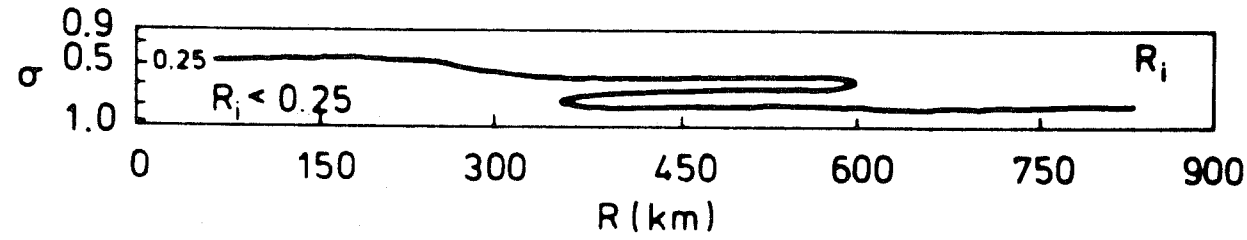

Figure 8 The Richardson number in the PBL of steady state hurricane.

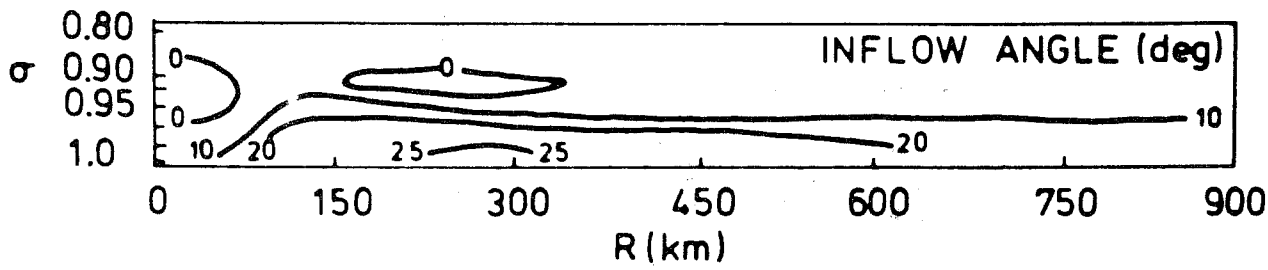

Figure 9 The inflow angle in the PBL of the steady state hurricane.

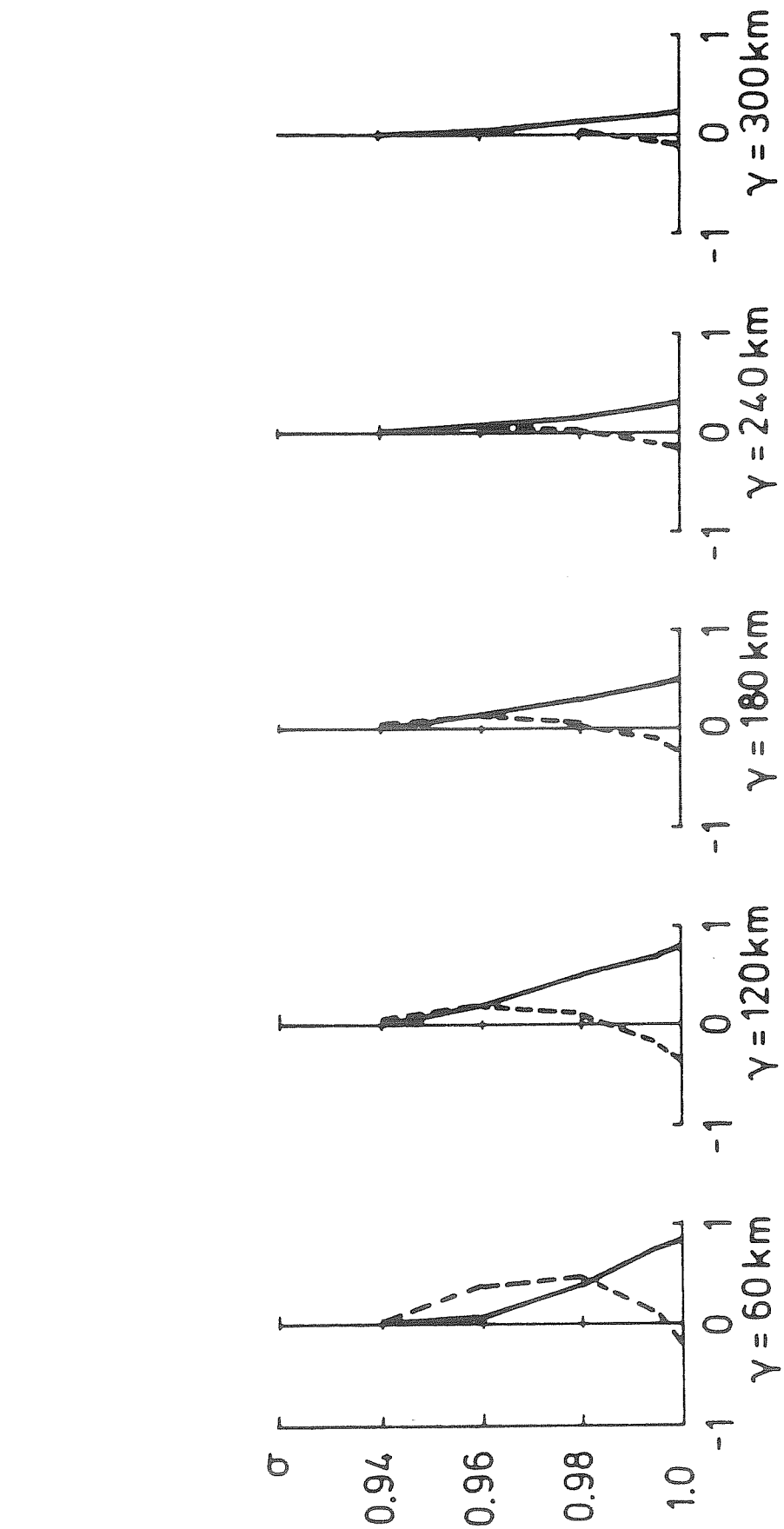

Figure 10 The steady state momentum fluxes in the tangential (solid line) and in the radial (broken line) direction at different radii.

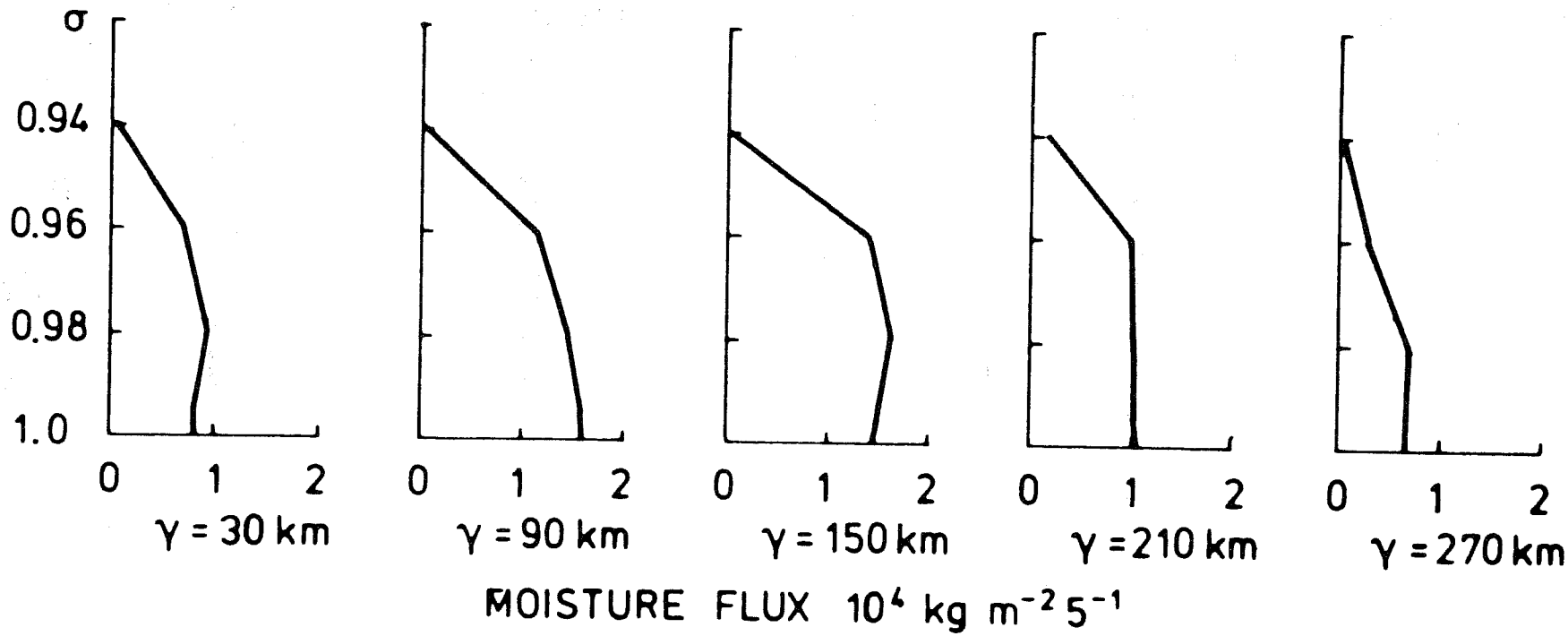

Figure 11 The steady state water vapour fluxes at different radii.

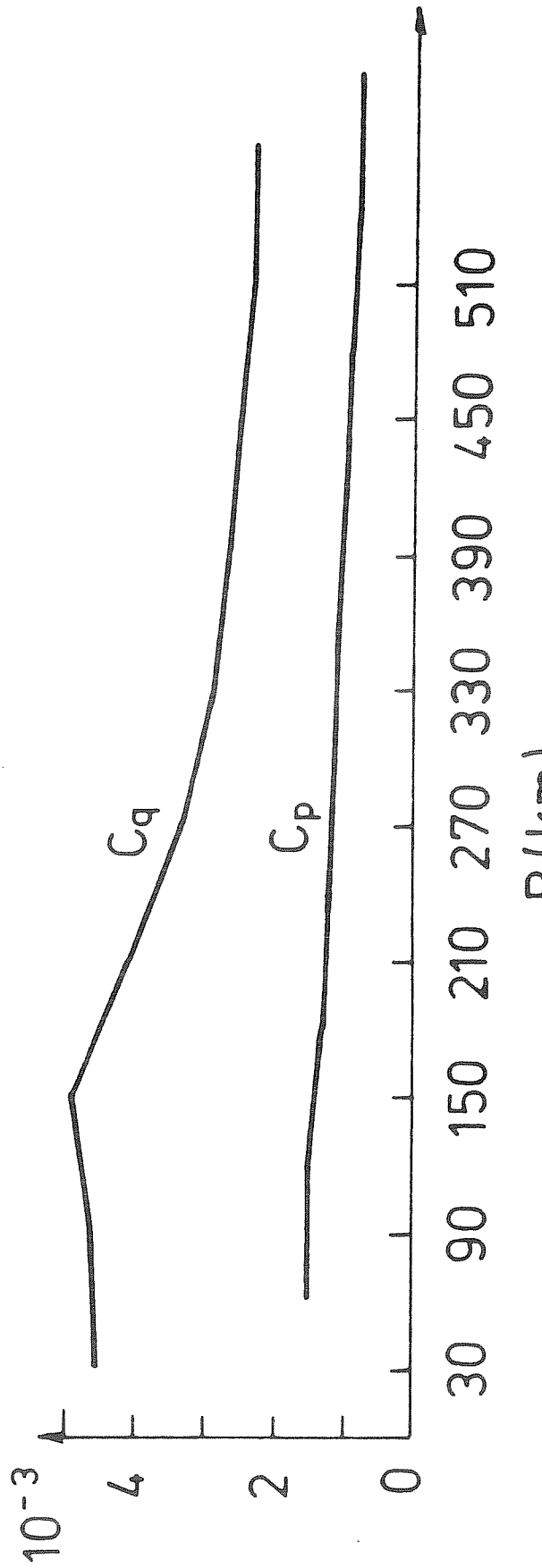

Figure 12 The equivalent drag coefficients for momentum (C_D) and water vapour (C_q) at steady state.

III. Reaction to Changed Ocean Surface Temperature

As summarized by Anthes (1974), the model hurricanes in general are very sensitive to the changes of the ocean surface temperature. The change of 1°C results in a 50% change of the maximum wind. In addition, the response to the changed ocean temperature takes place immediately after the temperature is changed. The rate of change is fastest in the first few hours after the change (e.g. Ooyamo, 1969).

Contrarily to those findings, our model hurricane shows a rather slow response to the change of ocean temperature. In addition, the rate of change from the steady state does not take place 12-24 h after the ocean temperature is changed.

In an experiment in which the ocean temperature is lowered by 1°C, the kinetic energy budget shows an immediate decrease of frictional dissipation rate. The low surface wind along with the development of a low level jet suggest a decoupling of the storm from the ocean surface. The water vapor budget also shows an immediate decrease of the evaporation, however, the effect of this decrease of latent energy supply is not felt in the first 6 h after the change of ocean temperature as shown by the fact that no significant decrease of storm intensity is detected. It is presumable that the decrease of frictional dissipation is large enough to allow the storm to maintain its intensity for several hours in spite of the reduction of the vapor supply. The storm intensity is rapidly reduced 12 h after the ocean temperature change by the decreased evaporation and decreased horizontal advection.

Various observations (e.g. Black and Withee, 1976) and model studies (O'Brien, 1967) suggest that ocean temperature is easily reduced by 1°C in 12 h by mechanical mixing under hurricane influence. The fact that the hurricanes are not weakened as they pass over a constantly cooled ocean substantiates our finding that the time scale for frictional dissipation to decrease is shorter than the time scale for the reduction in water vapor supply to be felt. Under typical condition, the intensity of a fast translating hurricane may not be affected by the cooled ocean surface at all.

Further experiments with a coupled ocean-hurricane model suggest that the storm weakening is further reduced by ocean feedback.

The result from an experiment in which the ocean temperature is increased by 1°C supports our postulation that the time scale for the frictional dissipation to increase is shorter than the time scale for the convective heating to enhance. If the hurricanes remain a long period of time over warmer ocean, then the explosive intensifications as mentioned by Namias (1973) are possible.

References

Anthes, R.A., 1971: Numerical experiment with a slowly varying model of the tropical cyclone. Mon. Wea. Rev. 99, 636-643.

Anthes, R.A., 1974: The dynamics and energetics of mature tropical cyclone. Rev. Geophysics Space Physics, 12, 495-522.

Black, P.G., and G. Withee, 1976: The effect of hurricane Eloise on the Gulf of Mexico. Sec. Conf. on Ocean-Atmosphere Interaction, Seatle, Washington.

Busch, N.E., S.W. Chang, and R.A. Anthes, 1976: A multo-layered model of the planetary boundary layer suitable for use with mesoscale dynamic model. J. Appl. Meteo., September.

Kuo, H.L., 1974: Further studies of the parameterization of the influence of cumulus convection on large scale flow. J. Atmos. Sci., 31, 1232-1240.

Namias, J., 1973: Weather note-birth of Hurricane Agnes - triggered by the transeguatorial movement of a mesoscale system into a favorable large-scale environment. Mon. Wea. Rev., 101, 177-179.

Nitta, T., 1975: Observational determination of cloud mass flux distributions. J. Atmos. Sci., 32, 73-91.

O'Brien, J.J., 1967: The non-linear response to a two-layer baroclinic ocean to a stationary, axially-symmetric hurricane: Part II. Upwelling and mixing induced by momentum transfer. J. Atmos. Sci., 24, 208-215.

Ooyama, K., 1969: Numerical simulation of the life-cycle of tropical cyclones. J. Atmos. Sci., 26, 3-40.

Rosenthal, S.L., and M.S. Moss, 1975: On the estimation of planetary boundary layer variables in mature hurricanes. Mon. Wea. Rev., 103, 980-988.

Sarachik, E.S., 1974: The tropical mixed layer and cumulus parameterization. J. Atmos. Sci., 31, 2225-2230.